Evidence from the Kyrenia Range, Cyprus, of the northerly active margin of the Southern Neotethys during Late Cretaceous–Early Cenozoic time

Geol. Mag.: page 1 of 27. © Cambridge University Press 2011
doi:10.1017/S0016756811000677

Evidence from the Kyrenia Range, Cyprus, of the northerly active margin of the Southern Neotethys during Late Cretaceous–Early Cenozoic time

ALASTAIR H. F. ROBERTSON*†, KEMAL TASLI‡ & NURDAN İNAN‡

*School of GeoSciences, University of Edinburgh, West Mains Road, Edinburgh EH9 3JW, UK
‡Department of Geology, Mersin University, Mersin 33343, Turkey

(*Received* 9 February 2010; *accepted* 25 January 2011)

Abstract – Sedimentary geology and planktonic foraminiferal biostratigraphy have shed light on the geological development of the northern, active continental margin of the Southern Neotethys in the Kyrenia Range. Following regional Triassic rifting, a carbonate platform developed during Jurassic–Cretaceous time, followed by its regional burial, deformation and greenschist-facies metamorphism. The platform was exhumed by Late Maastrichtian time and unconformably overlain by locally derived carbonate breccias, passing upwards into Upper Maastrichtian pelagic carbonates. In places, the pelagic carbonates are interbedded with sandstone turbidites derived from mixed continental, basic volcanic, neritic carbonate and pelagic lithologies. In addition, two contrasting volcanogenic sequences are exposed in the western-central Kyrenia Range, separated by a low-angle tectonic contact. The first is a thickening-upward sequence of Campanian–Lower Maastrichtian(?) pelagic carbonates, silicic tuffs, silicic lava debris flows and thick-bedded to massive rhyolitic lava flows. The second sequence comprises two intervals of basaltic extrusive rocks interbedded with pelagic carbonates. The basaltic rocks unconformably overlie the metamorphosed carbonate platform whereas no base to the silicic volcanic rocks is exposed. Additional basaltic lavas are exposed throughout the Kyrenia Range where they are dated as Late Maastrichtian and Late Paleocene–Middle Eocene in age. In our proposed tectonic model, related to northward subduction of the Southern Neotethys, the Kyrenia platform was thrust beneath a larger Tauride microcontinental unit to the north and then was rapidly exhumed prior to Late Maastrichtian time. Pelagic carbonates and sandstone turbidites of mixed, largely continental provenance then accumulated along a deeply submerged continental borderland during Late Maastrichtian time. The silicic and basaltic volcanogenic rocks erupted in adjacent areas and were later tectonically juxtaposed. The Campanian–Early Maastrichtian(?) silicic volcanism reflects continental margin-type arc magmatism. In contrast, the Upper Maastrichtian and Paleocene–Middle Eocene basaltic volcanic rocks erupted in an extensional (or transtensional) setting likely to relate to the anticlockwise rotation of the Troodos microplate.

Keywords: Kyrenia Range, Cyprus, Neotethys, Upper Cretaceous–Palaeogene, sedimentology, biostratigraphy.

1. Introduction

The elongate Kyrenia Range in the northern part of Cyprus, also known as the Beşparmak Range in Turkish and the Pentadaktylos Range in Greek (Fig. 1), documents the tectonic, sedimentary, magmatic and metamorphic development of the northern, active continental margin of a southerly Neotethyan ocean basin (Southern Neotethys) during Late Cretaceous–Early Cenozoic time (Robertson & Dixon, 1984; Dercourt *et al*. 1986, 2000; Robertson, 1998; Barrier & Vrielynck, 2009). The axis of the western and central segments of the Kyrenia Range is dominated by Triassic to Cretaceous platform carbonates whereas the eastern range crest and the Karpas Peninsula are characterized by Palaeogene pelagic carbonates and volcanic rocks, in turn overlain by Middle Eocene sedimentary melange ('olistostromes'; Fig. 1). The flanks of the range are largely Neogene and Plio-Quaternary sedimentary deposits (Henson, Brown & McGinty, 1949; Ducloz, 1972; Cleintuar, Knox & Ealey, 1977; Baroz, 1979; Robertson & Woodcock, 1986; Kelling *et al*. 1987; Stampfli & Borel, 2002; Zitter, Woodside & Mascle, 2003; Harrison *et al*. 2004; G. McCay, unpub. Ph.D. thesis, Univ. Edinburgh, 2010; Fig. 1).

The Kyrenia Range developed in four main phases: Late Cretaceous; Middle Eocene; Late Miocene–Early Pliocene and Late Pliocene–Recent (Robertson & Woodcock, 1986). The Late Cretaceous phase has remained enigmatic, with both large-scale thrusting and strike-slip faulting suggested to play an important role (Baroz, 1979; Robertson & Woodcock, 1986). Southward thrusting took place during Middle Eocene time (Baroz, 1979; Robertson & Woodcock, 1986). Uplift of the Kyrenia Range mainly took place during Late Pliocene–Quaternary time. The main controls of uplift were subduction beneath Cyprus, collision of the Eratosthenes Seamount with the Cyprus trench and the westward tectonic escape of Anatolia towards

†Author for correspondence: Alastair.Robertson@ed.ac.uk

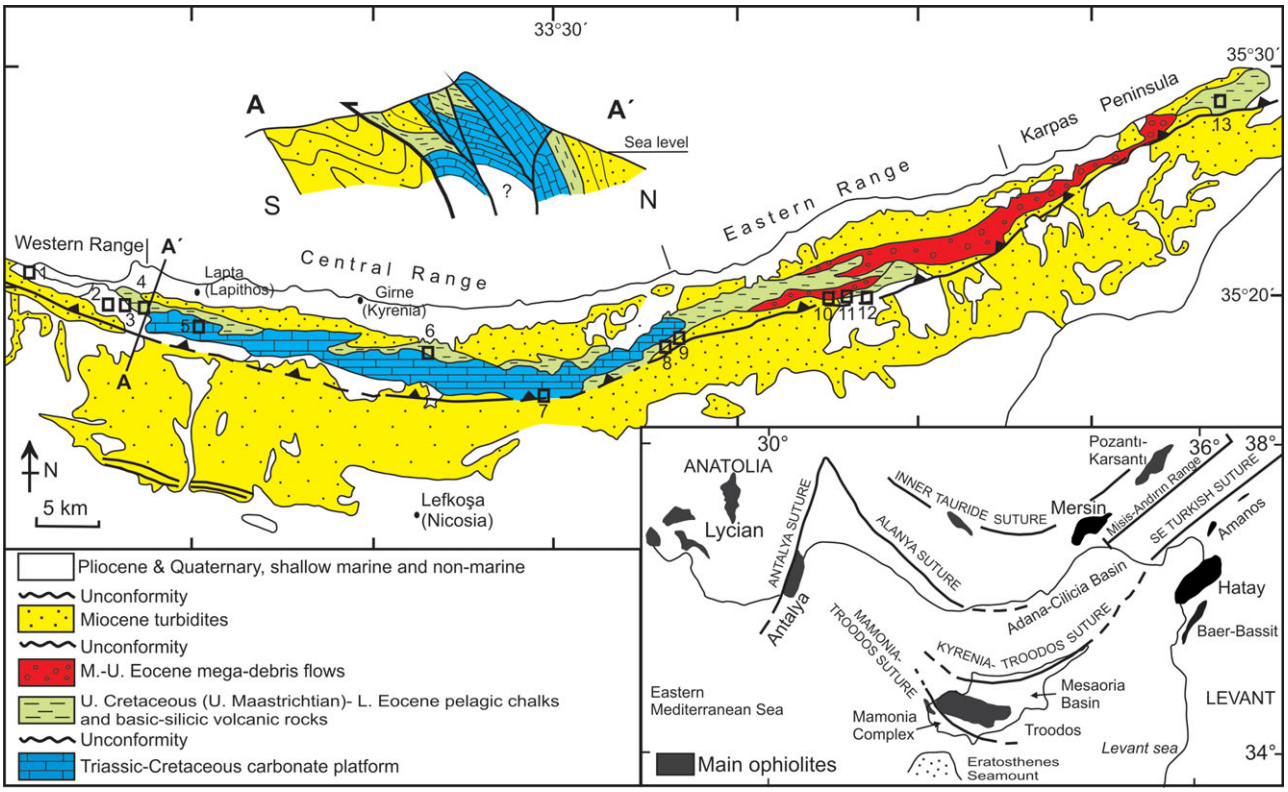

Figure 1. (Colour online) Regional geological setting of the Kyrenia Range in the northern part of Cyprus. Outline map based on Baroz (1979) and Robertson & Woodcock (1986). Upper left: Simplified cross-section of the Kyrenia Range, modified from Baroz (1979) and Robertson & Woodcock (1986). Below right: Setting in the Eastern Mediterranean, showing the main sutures and the Upper Cretaceous ophiolites. Locations for which new microfossil data are given here are numbered on the map, with small boxes. 1 – Kayalar (Orga), 2 – Geçiköy (Panagra), 3 – Selvilitepe (Fourkovouno), 4 – Karşıyaka (Vassilea), 5 – Alevkaya Tepe (Kiparisso Vouno), 6 – Beylerbey (Bellapais), 7 – Değirmenlik (Kithrea), 8 – Ergenekon (Ayios Chariton), 9 – Tirmen (Trypimeni), 10 – Mallıdağ (Melounda), 11 – Çınarlı (Platani), 12 – Ağıllar (Mandes), 13 – Balalan (Platanisso).

the Aegean region (Robertson, 1998; Kempler & Garfunkel, 1994; Kempler, 1998; Harrison *et al.* 2004).

This paper focuses on the Late Cretaceous–Palaeogene development of the Kyrenia Range. An important unconformity exists between a deformed and metamorphosed Mesozoic carbonate platform below, and an unmetamorphosed, mixed pelagic carbonate, siliciclastic and volcanogenic succession, above. We also consider the volcanology, age and structural setting of Upper Cretaceous and Palaeogene volcanic rocks, especially those exposed in the western range. Pelagic carbonates that are closely associated with the volcanic rocks were collected throughout the Kyrenia Range for biostratigraphic dating mainly using planktonic foraminifera. Samples were initially selected for sampling using a high-power hand lens (× 20). Multiple samples (up to four) were collected from the same locality in most cases. The zonal scheme of Robaszynski & Caron (1995) was used for the Upper Cretaceous and the ranges given by Sartorio & Venturini (1988) for the Cenozoic. Chemical analyses were previously obtained for the Upper Cretaceous and Palaeogene volcanic rocks throughout the Kyrenia Range (Pearce, 1975; Robertson & Woodcock, 1986; Huang, Malpas & Xenophontos, 2007; K. Huang, unpub. M.Sc. thesis, Univ. Hong Kong, 2008) and these results are integrated here.

Taken together, the available evidence provides the basis of a new tectonic model for the Late Cretaceous–Palaeogene tectonic development of the Kyrenia Range, with implications for the wider development of the Neotethys.

Additional illustrations of the igneous and sedimentary rocks are published in an online Appendix at http://journals.cambridge.org/geo.

2. Late Cretaceous deformation and metamorphism

An unconformity was mapped in the western and central Kyrenia Range between metamorphosed and recrystallized Triassic–Cretaceous platform carbonates of the Trypa (Tripa) Group (Fig. 2) and unmetamorphosed Upper Cretaceous–Palaeogene pelagic carbonates and volcanic rocks of the overlying Lapithos (Lapta) Group (Fig. 1, cross-section; Fig. 3a–c). Carbonate rocks beneath the unconformity are mainly massive, coarsely crystalline marbles. These locally retain primary sedimentary structures (e.g. microbial lamination) indicative of deposition on a shallow-water carbonate platform. Intercalations of muscovite schist, pelitic schist and phyllite, commonly dark

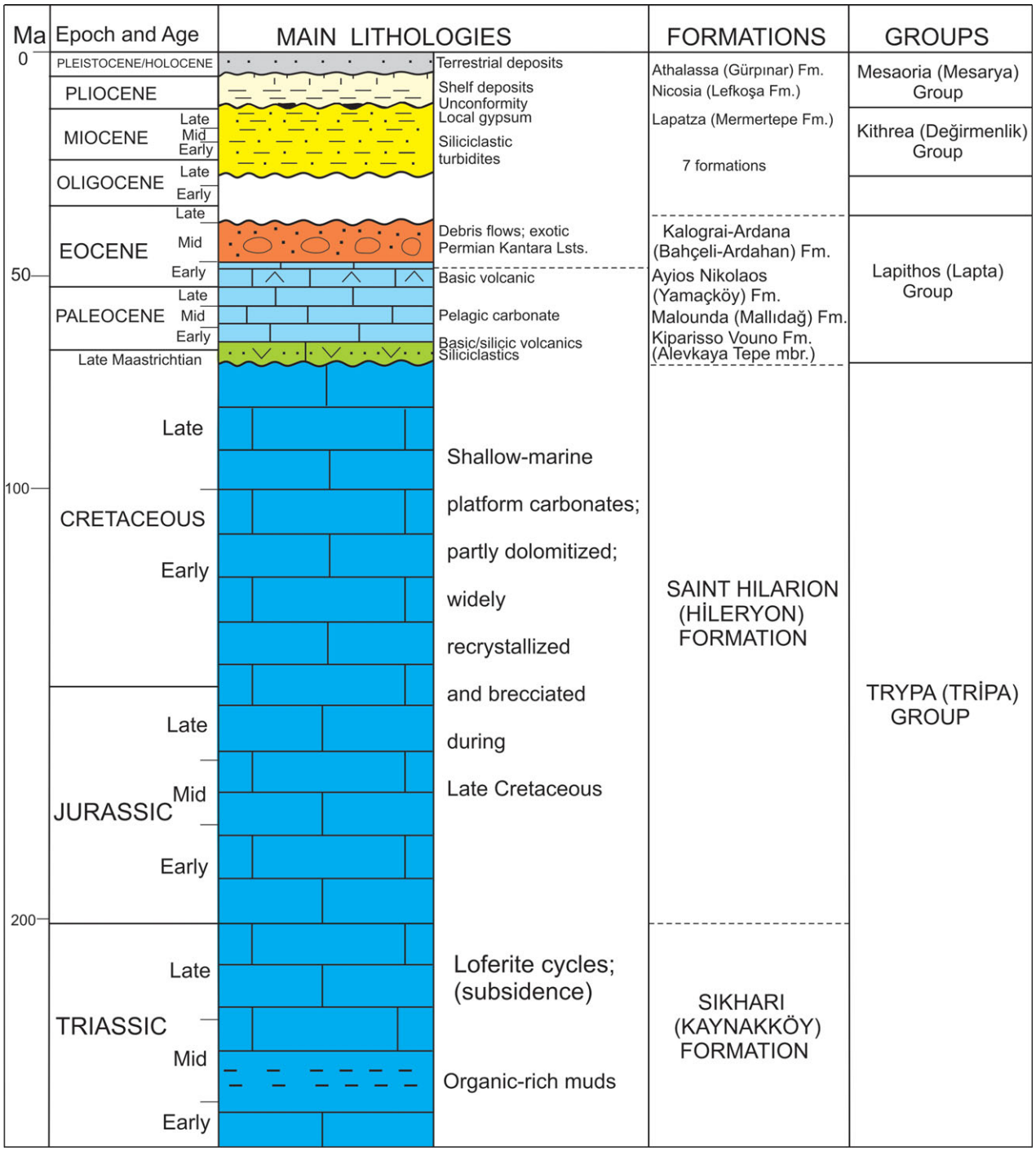

Figure 2. (Colour online) Age, main lithologies and stratigraphy of units exposed in the Kyrenia Range. In this paper, the initially defined Greek stratigraphic names are used, with the Turkish equivalents in parentheses. Data from Henson *et al*. (1949), Ducloz (1972), Baroz (1979), Robertson & Woodcock (1986) and Hakyemez *et al*. (2000).

and graphitic, are also locally exposed beneath the unconformity, as seen in the western part of the central Kyrenia Range (e.g. near Alevkaya Tepe (Kiparisso Vouno); Area 5 in Fig. 1).

The limestones and dolomites of the Trypa (Tripa) Group are commonly brecciated to form a characteristic jigsaw texture. Adjacent clasts have undergone little or no transport relative to each other (Robertson & Woodcock, 1986; Fig. 4a). The brecciation is well developed close to the unconformity and the breccias have contributed material especially to the basal facies above the unconformity (Fig. 4c).

The brecciated and metamorphosed Mesozoic carbonate platform is unconformably overlain by unmetamorphosed pelagic carbonates in the western and central range (Fig. 2). Exposures along the northern flank of the central range can be traced laterally for $\sim$ 20 km within a single large thrust sheet that dominates this part of the Kyrenia Range. The unconformity surface is highly irregular, with angular protrusions

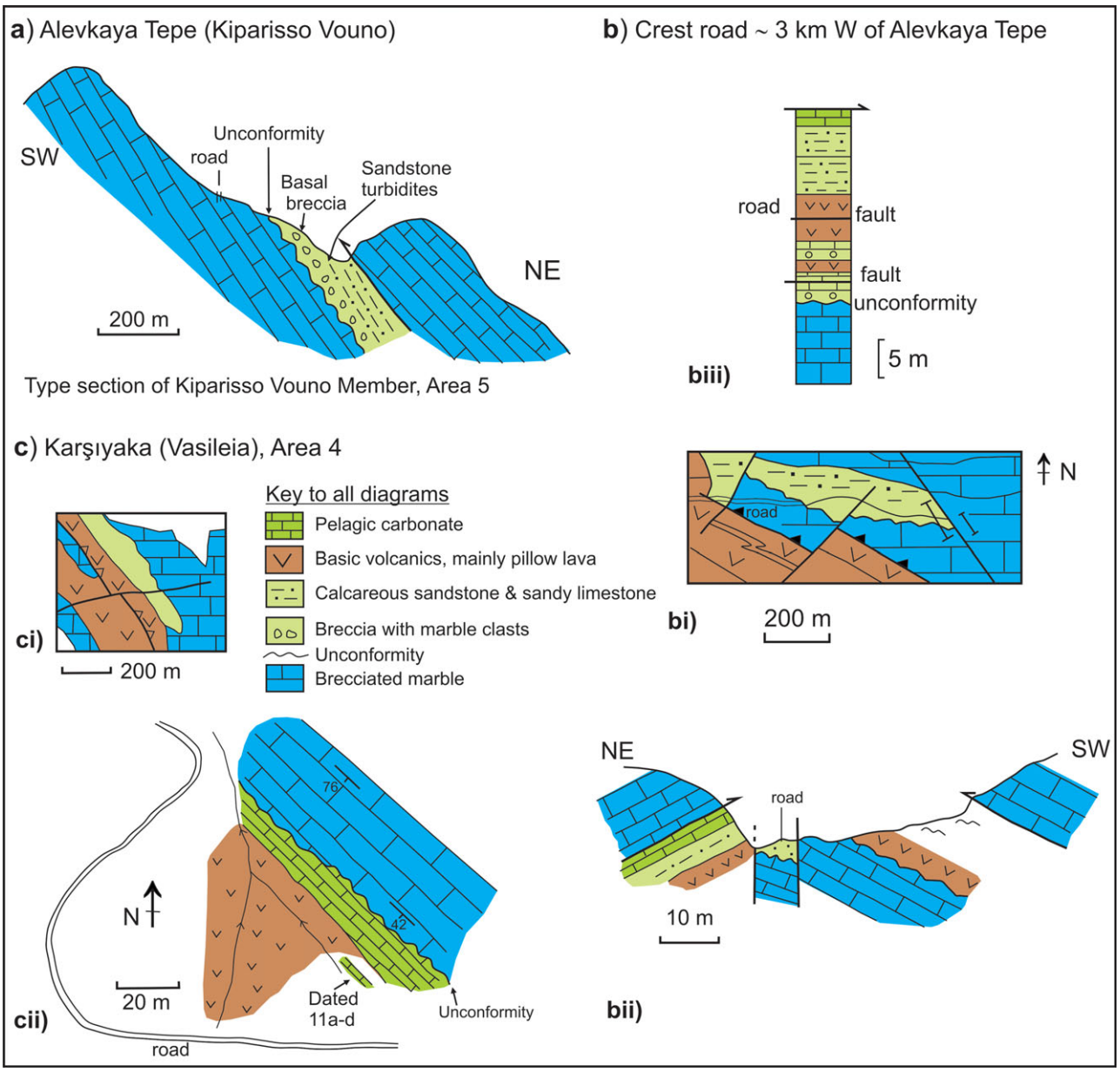

Figure 3. (Colour online) Field relations of the Upper Cretaceous Kiparisso Vouno (Alevkaya Tepe) Member of the Melounda (Mallıdağ) Formation, as defined here (see Fig. 2). (a) Profile of the type section on the north flank of Alevkaya Tepe (Kiparisso Vouno Mountain), in a wooded depression below the crest road. The section, which is poorly exposed, begins with tectonically brecciated crystalline limestone and dolomite (marble). The overlying unconformity is followed by a basal breccia of marble clasts in a matrix of pink pelagic carbonate. Rare clasts of calc-mylonite and calc-schist are also present. The succession continues with sandstone turbidites interbedded with shale and is then overthrust by a higher-level thrust sheet dominated by dark organic-rich, brecciated loferite-type marble of the Trypa (Tripa) Group. (bi) Sketch map showing the occurrence of calcareous sandstone and sandy limestone turbidites of the Kiparisso Vouno (Alevkaya Tepe) Member further west along the crest of the Kyrenia Range, 2.5 km east of Kornos Mountain; modified from Baroz (1979). (bii) Local cross-section showing the Upper Cretaceous transgression over the St Hilarion (Hileryon) Formation, cut by sub-vertical faults and overthrust by a higher-level thrust sheet of Hilarion marble. (biii) Log showing the Upper Cretaceous succession at map locality (bi). (ci) Sketch map (based on Baroz, 1979) showing part of the unconformity between the Hilarion (Hileryon) Formation and the Upper Cretaceous cover. (cii) Larger scale sketch map of part of the area in (ci) showing the Hilarion marble unconformably overlain by a basal breccia made up of angular to sub-angular marble clasts in a pink pelagic matrix, followed by pink pelagic carbonate and pillow basalt.

and declivities surrounded and filled in by pink pelagic limestone (Fig. 4b). Pink carbonate penetrates down into fissures in the underlying marble for up to several metres. The bedding in the meta-carbonates and cover, where observable, is sub-parallel in local outcrops but maps out as a low-angle discordance ($< 20^{\circ}$).

The pelagic carbonates just above the unconformity surface are commonly packed with angular clasts of pale grey to dark grey marble (Selvilitepe Breccia of Hakyemez *et al*. 2000). These breccias have been reported to pass laterally into the Mallıdağ (Melounda) Formation that has been dated as Late Maastrichtian in age (Hakyemez & Özkan-Altıner, 2007). Overlying

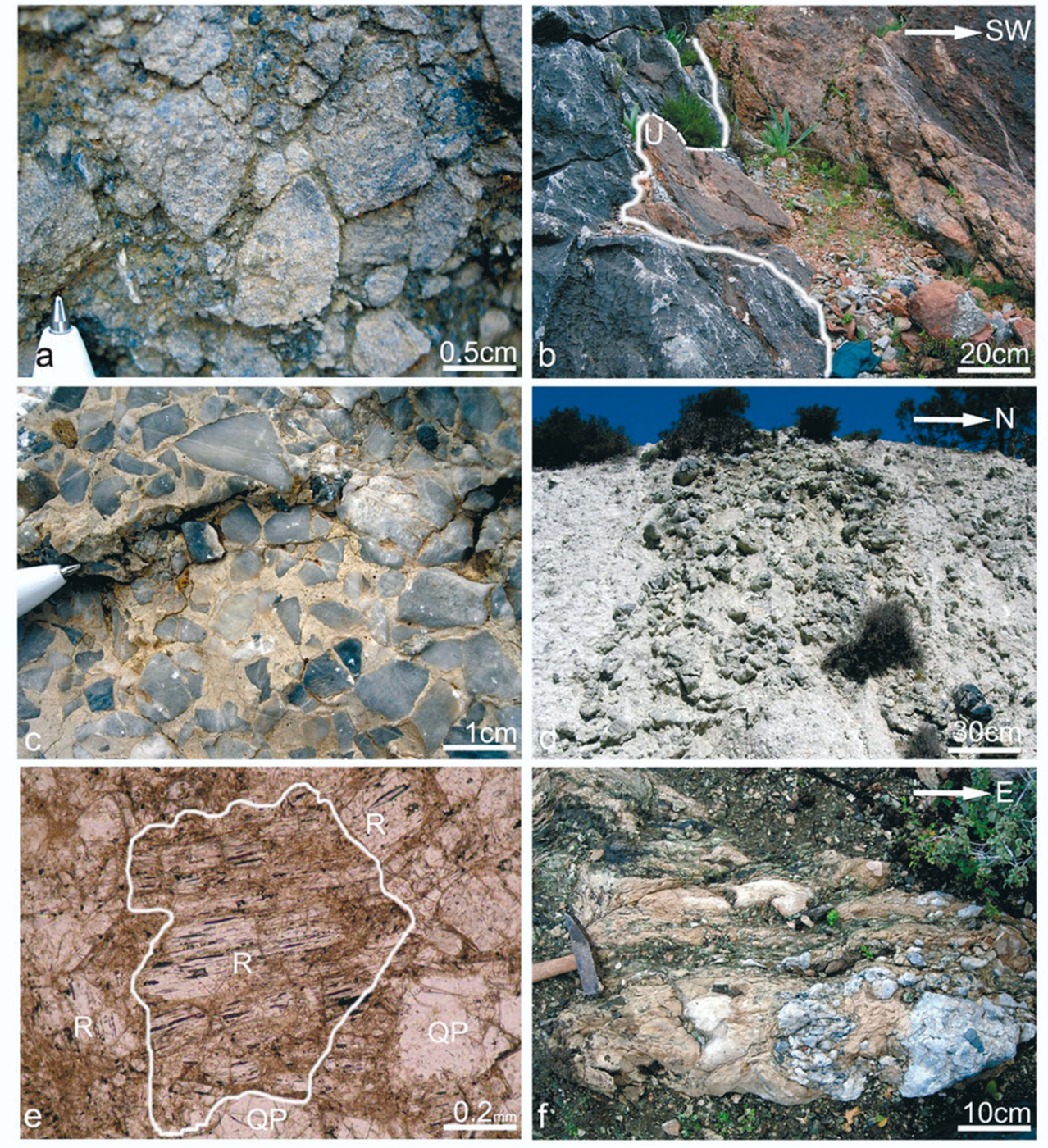

Figure 4. (Colour online) Field photographs and photomicrograph. (a) Tectonic breccia within marble of the St Hilarion (Hileryon) Formation, as commonly developed in the metamorphosed Mesozoic carbonate platform of the Kyrenia Range. Angular fragments form an interlocking jig-saw-type fabric with little or no matrix; from beneath the unconformity with the Upper Cretaceous Melounda (Mallıdağ) Formation; locality 5 on Fig. 1. (b) Irregular unconformity between thick-bedded marble of the St Hilarion (Hileryon) Formation and pink basal breccia and pelagic carbonate of the Melounda (Mallıdağ) Formation (unconformity U marked by solid line); angular clasts of marble (grey) occur just above the unconformity surface; locality 4 on Figure 1. (c) Basal breccia of the Upper Cretaceous Mallıdağ (Melounda) Formation made up of angular clasts of grey crystalline limestone (marble) in an off-white matrix of unrecrystallized pelagic carbonate containing *Globotruncana* sp. and other Upper Cretaceous microfossils; locality 5 on Figure 1. (d) Steeply dipping debris flow made up of mainly sub-rounded boulders of reworked rhyolite in a matrix of silicic tuff; road section 0.7 km north of Geçiköy (Panagra); locality 2 on Figure 1. (e) Outlined grain of silicic glass (isotropic) within silicic tuff. The glass includes numerous elongate gas and fluid inclusions (viewed in plane-polarized light). Abbreviations: R – rhyolite; QP – quartz phenocryst. (f) Upper Cretaceous pelagic chalk (pink) with angular to sub-angular clasts of marble (grey) derived from the Hileryon (St Hilarion) Formation. The pelagic limestone is interbedded with altered silicic tuff and includes *Globotruncana* sp.; from the upper part of the sequence exposed 1.5 km west of Kayalar (Orga); locality 1 on Figure 1 (see also Fig. 10).

pink pelagic limestone locally contains interbeds of sedimentary breccia up to 1 m thick. The clasts include pale grey marble derived from the St Hilarion (Hileryon) Formation and dark grey meta-dolomite from the Sikhari (Kaynakköy) Formation (Fig. 2). Clasts are mainly angular, < 5 cm in size and set in a pink pelagic matrix rich in planktonic foraminifera.

Four samples of pelagic carbonates associated with the basal breccias were collected from just above the unconformity (near Karşıyaka (Vasileia); Fig. 3cii) and dated as Late Maastrichtian (samples 06/11a–d) (see Table 1).

The unconformity marks a regional structural and metamorphic break. The Mesozoic carbonate platform, estimated as at least several kilometres thick (Baroz, 1979; Robertson & Woodcock, 1986), was deeply buried, metamorphosed, exhumed and then covered by pelagic carbonate and talus derived from the metamorphosed carbonate platform beneath. Taking account of the occurrence of pelitic rocks throughout the Kyrenia Range and the persistence of chlorite and stilpnomelane, Baroz (1979) estimated the burial temperature as up to 450 °C (greenschist facies). The peak metamorphic pressure remains unconstrained in the absence of a diagnostic mineral assemblage. In principle the unconformity could be explained by erosion or tectonic exhumation of the carbonate platform. The second option is preferred because (1) the greenschist-facies metamorphism implies at least several kilometres of burial of the carbonate platform but there is little erosional detritus above the unconformity; (2) the basal overlying sediments are pelagic carbonates with no evidence of subaerial exposure; (3) tectonic breccias below the unconformity were reworked as texturally immature (angular) material directly above the unconformity.

The Kyrenia Range carbonate platform rocks were therefore exhumed and exposed on the seafloor in a submarine, pelagic-depositing setting by Late Maastrichtian time. The talus above the unconformity mainly accumulated by debris-flow and rock fall processes indicating the existence of a rugged seafloor topography.

The timing of the deformation and metamorphism are only loosely constrained because the meta-carbonate platform has so far yielded only Triassic and Late Jurassic ages (Ducloz, 1972; Baroz, 1979; Robertson & Woodcock, 1986; Hakyemez *et al*. 2000). Further north, parts of the Tauride carbonate platform were deformed by thrusting and folding during Late Cretaceous time but remained regionally unmetamorphosed (e.g. Robertson, 1998) in contrast to the Kyrenia Range.

3. Maastrichtian sedimentation

Above the unconformity, contrasting Upper Cretaceous successions are exposed in several parts of the western and central Kyrenia Range.

3.a. Type area in the western Range

Upper Cretaceous clastic sediments are exposed in a regionally persistent thrust sheet of meta-carbonates that dominates the northern flank of the western and central range (Fig. 1, cross-section). In some sections the Upper Maastrichtian carbonate breccias and basal pelagic carbonates pass upwards into calcareous sandstones and sandy calcarenites. Similar sandstones were previously recognized locally in the central Kyrenia Range, where they were termed the Kiparisso Vouno Formation by Baroz (1979; Fig. 2). A Late Cretaceous age (Late Campanian) was suggested based on planktonic foraminifera within 'associated' pelagic carbonates. Baroz (1979) was unsure if the contact with the underlying Trypa Group was depositional or tectonic. Robertson & Woodcock (1986) inferred the contact to be depositional but field relations remained unclear. Hakyemez *et al*. (2000) later included clastic sediments that appear to be equivalent to the Kiparisso Vouno Formation of Baroz (1970) within a zone of imbricated thrust sheets exposed near Alevkaya Tepe (Kiparisso Vouno). These critical field relations were clarified during this work.

The unconformity between the recrystallized neritic carbonates of the St Hilarion (Hileryon) Formation and the Upper Cretaceous cover succession (Lapithos (Lapta) Group) was mapped discontinuously for ∼ 20 km within a single thrust sheet. This is exposed along the northern flank of the western part of the central Kyrenia Range (east and west of Area 5 in Fig. 1). The 'Kiparisso Vouno Formation' was found to be a stratigraphic intercalation within the Melounda (Mallıdağ) Formation. Baroz's (1979) Kiparisso Vouno Formation is, therefore, here redefined as the Kiparisso Vouno (Alevkaya Tepe) Member of the Melounda (Mallıdağ) Formation (Fig. 2).

Details of the type section of the Kiparisso Vouno (Alevkaya Tepe) Member are given in Figure 3a.

Basal sedimentary breccias are dominated by angular clasts of recrystallized limestone and psammitic metamorphic rocks, together with polycrystalline quartz and rare grains of muscovite schist (Fig. 5a). Medium-grained calcareous sandstone and shales (∼ 25 m thick) are seen above this, although exposure is poor. Sandstones (Fig. 5b) studied in five thin-sections are compositionally similar, mainly made up of marble, recrystallized dolomite, polycrystalline quartz (paraquartzite), unstrained quartz (of probable plutonic origin) and muscovite schist (locally folded). Rare grains of micrite contain occasional planktonic foraminifera (unrecrystallized), thin-walled shell fragments and altered basalt (mainly as rounded lumps). There are also scattered grains of biotite, plagioclase and chloritized lava. Rare small grains of tourmaline, epidote, sphene and phrenite are also present. Sparse grains of altered diabase (with intersertal plagioclase), pyroxene, altered basalt (with feldspar microphenocrysts) and microcrystalline quartz (recrystallized chert) are also seen. Several samples include

Table 1. Summary of the main Upper Cretaceous species of planktonic and benthic foraminifera identified during this study, utilizing the biozonation scheme of Robaszynski & Caron (1995)

SAMPLE NUMBER*	CHRONOSTRATI-GRAPHY	*Contusotruncana contusa* (Cushman)	*Abatomphalus mayaroensis* (Bolli)	*Gansserina gansseri* (Bolli)	*Rugoglobigerina scotti* (Brönnimann)	*Rugoglobigerina* sp.	*Globotruncanita stuarti* (De Lapparent)	*Globotruncana falsostuarti* Sigal	*Globotruncanita stuartiformis* (Dalbiez)	*Globotruncana arca* (Cushman)	*Contusotruncana fornicata* (Plummer)	*Globotruncanita conica* (White)	*Globotruncanita* sp. (reworked)	*Orbitoides* sp. (reworked)	*Pseudosiderolites* sp. (reworked)	Globotruncanidae indet.
06/10a	UPPER MAASTRICHTIAN	Fig.6f					Fig.6j		X	X						
06/11a		Fig.6g		X		X	X	Fig.6c		X	X					
06/31b		X						X	X	X	X					
06/21b			Fig.6h	X		Fig.6a	X									
06/29b			X					X				X				
06/30			X		X		X									
09/40			X	X				X		X						
249			X					X								
06/3a				Fig.6d2		X	X									
06/4a				X			X				X					
06/8a				X			X			X						
06/10b				X		X						X				
06/11b				X		X	X									
06/11d				Fig.6d1		X		X	Fig.6i	X	Fig.6e					
06/21a				X		X										
06/27a				X				X	X	X						
09/41				X					X							
09/47				X				X								
06/2a					Fig.6b	X	X	X		X	X					
06/17a					X											
06/17b					X											
06/17c					X		X									
06/17e					X											
06/28a					X		X									
06/28b					X		X		X							
06/11c						X	X	X		X	X					
06/17d						X										
06/21c						X	X									
06/1a	UPPER CAMPANIAN–MAASTRICHTIAN						X	X		X	X					
06/29a							X									
06/31a							X	X			X					
09/28							X	X								
250							X				X					
09/21								X		X						
09/32								X	X		X					
09/18													X	X	X	
09/19														X		
06/26a	UPPER CRETACEOUS															X

*See Appendix Table A1 for location data.

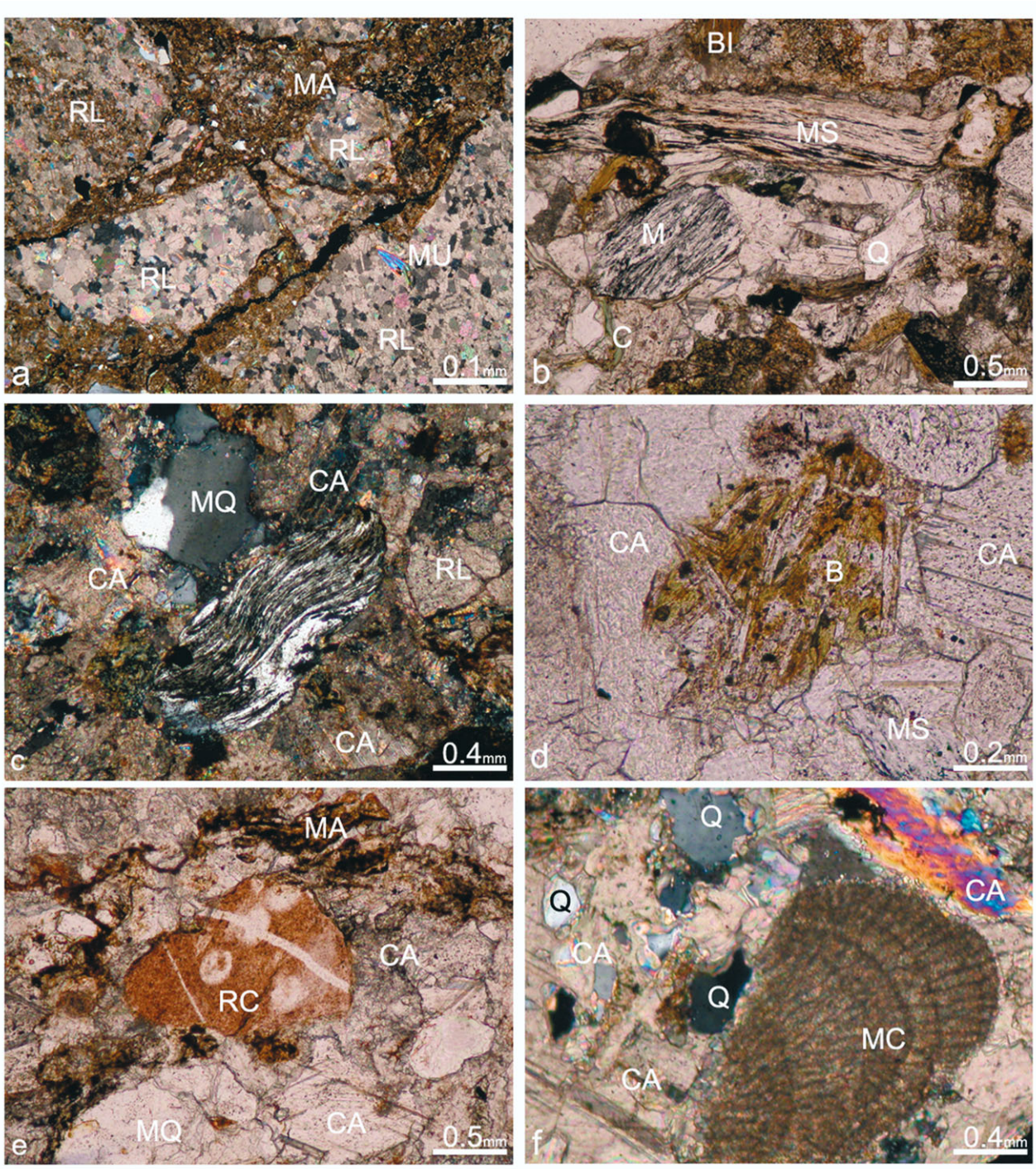

Figure 5. (Colour online) Photomicrographs of grains within sandstone turbidites of the Maastrichtian Kiparisso Vouno (Alevkaya Tepe) Member. (a) Basal breccia. Angular clasts of recrystallized limestone (marble) derived from the St Hilarion (Hileryon) Formation, with a matrix of ferruginous and calcareous siltstone; base of type section of the Kiparisso Vouno (Alevkaya Tepe) Member of the Melounda (Mallıdağ) Formation; locality 5 on Fig. 1. (b) Schist grains together with quartz, biotite, chlorite and calcite spar cement; upper level of the Kiparisso Vouno (Alevkaya Tepe) Member type section; same locality as (a). (c) Detrital grains including folded mylonite and metamorphic quartz (polycrystalline quartz) with a calcite spar cement. From calcareous sandstone turbidites interbedded with more carbonate-rich turbidites and pelagic carbonates; facies equivalent of the Kiparisso Vouno (Alevkaya Tepe) Member; locality 4 on Fig. 1. (d) Detrital grain of basalt with feldspar microphenocrysts in a mesostasis of chloritized glass; set with other detrital grains in a calcite spar cement; same locality as (c). (e) Detrital grains of radiolarian chert and metamorphic quartz within a sparse muddy matrix showing pressure solution cleavage together with a calcite spar cement; same locality as (c). (f) Detrital grains of microbial carbonate (calcareous algae) and quartz in a calcite spar cement; same locality as (c). Abbreviations: B – basalt with feldspar microphenocrysts; BI – biotite, CA – calcite cement; MA – matrix, M – mylonite (folded); MC – microbial carbonate; MI – mylonitic schist; MS – muscovite schist; MQ – metamorphic quartz (quartzite), MU – muscovite; RC – radiolarian chert; RL – recrystallized limestone (marble); Q – quartz.

numerous grains of microbial carbonate, micritic limestone with planktonic foraminifera (e.g. reworked Heterohelicidae), rare benthic foraminifera and shell fragments.

Comparable sandstones were observed ∼ 1 km westwards on strike from the type section in a small area that straddles the range crest road (Fig. 3bi, bii). These sandstones are correlated with the Kiparisso Vouno (Alevkaya Tepe) Member. They are interbedded with pelagic carbonates of the Melounda (Mallıdağ) Formation that contain a rich assemblage of Upper Cretaceous planktonic foraminifera (Fig. 3biii; Fig. 6f, m). Elsewhere, the Melounda (Mallıdağ) Formation as a whole has been dated as Late Maastrichtian in age (Hakyemez *et al*. 2000). Hemipelagic carbonates are interbedded with fine- to medium-grained, thin- to medium-bedded calcareous sandstones and sandy calcarenites (∼ 10 m thick). These contain abundant grains of marble, quartz, metamorphic quartz and muscovite schist (rarely folded), together with rare, angular fragments of altered basalt and red radiolarian chert (angular to sub-rounded), rare finely crystalline grey serpentinite, green chloritic grains, red mudstone and rare plagioclase (with microlitic inclusions), pyroxene, feldspar and biotite (Fig. 5c–f). The matrix is micritic, with scattered echinoderm plates, rare planktonic foraminifera (including Globotruncanidae) and microbial carbonate. Pelagic carbonate follows then the succession is truncated by a thrust (Fig. 3biii).

The Upper Cretaceous succession (Fig. 3a, b) can be traced westwards for ∼ 3 km within the same large thrust sheet to Area 4 (Karşıyaka (Vasileia)) on the lower northern flanks of the range. However, Upper Maastrichtian sandstone turbidites of the Kiparisso Vouno (Alevkaya Tepe) Member are absent in this area (Fig. 3cii).

Where present, the turbidites of the Kiparisso Vouno (Alevkaya Tepe) Member appear to have filled in seafloor depressions in the unconformity surface rather than forming a laterally continuous blanket above the Mesozoic meta-carbonate platform. The clastic sediment was mainly derived from continental crust, in the form of quartz, schist and marble, together with minor neritic and pelagic carbonate.

The obvious source of the Upper Maastrichtian clastic sediments is the underlying metamorphosed carbonate platform that includes schistose and pelitic intercalations. However, the detrital grains are relatively fine and well sorted suggesting a distal source in contrast to the basal carbonate breccias. The basalt is unrepresented in the Trypa (Tripa) Group. Also, the neritic carbonate grains (microbial carbonate; benthic foraminifera; shell fragments) indicate a shallow-marine setting that is not known in the Maastrichtian of the Kyrenia Range. On the other hand, the intraclasts of pelagic carbonate were probably reworked from the local Upper Maastrichtian pelagic succession.

3.b. Comparable exposures

Baroz (1979) mentions one other outcrop of his Kiparisso Vouno Formation, which is on the northern flank of the central range at the same structural level as the type section further west (Fig. 1, Area 6). After a search, a small outcrop described by Baroz (1979) was located within a small stream valley above cliffs (accessible only from above), southeast of Beylerbey (Bellapais) (Fig. 7a). Baroz (1979) mapped Upper Cretaceous clastic sediments faulted against marbles of the St Hilarion (Hileryon) Formation (to the south). These were shown as being depositionally overlain by Palaeogene pelagic carbonates of the Ayios Nicolaos (Yamaçköy) Formation (to the north). However, several differences were noted during this work (Fig. 7b). Massive to crudely bedded marbles of the St Hilarion (Hileryon) Formation dip steeply southwards and are in thrust contact with a thin sliver of altered basalt, above (Fig. 7b). This is tectonically overlain by a short interval of sandstone and microconglomerate, only several metres thick. Baroz (1979) reported a conformable upwards transition from Upper Cretaceous clastic sediments to Palaeogene pelagic chalks. However, the clastic and pelagic sediments are separated by a shear plane. The overlying pelagic chalk contains well-preserved planktonic foraminifera of Late Paleocene age (see Fig. 6q1, q2; Table 2).

Fine-grained calcareous sandstones near the base of the local succession contain quartz, polycrystalline (metamorphic quartz), mica schist, rare plagioclase, rare chlorite and numerous planktonic foraminifera, also sparse, reworked planktonic foraminifera dated as Late Campanian–Maastrichtian in age (sample K/09/21; see Table 1). Coarser sandstones and pebblestones above this include abundant grains and clasts of metamorphic rocks (marble, polycrystalline quartz, mica schist), igneous rocks (fresh and altered basalt, pyroxene, serpentinite) and both pelagic and neritic sedimentary rocks (e.g. variably recrystallized radiolarian chert). Some chert grains and pebbles are moderately to well rounded suggesting extended transport prior to deposition. Illustrations are shown in the online Appendix at http://journals.cambridge.org/geo.

Additional exposures on the hillside further southeast (∼ 1 km SE of Beylerbey (Bellapais; Fig. 7a) were not mentioned by Baroz (1979). Pelagic carbonate there is interbedded with silty marl and thin- to medium-bedded, fine- to medium-grained, graded sandstones and pebblestones (in a ∼ 2.5 m thick exposure). These sediments overlie a large, laterally persistent thrust sheet of Mesozoic meta-carbonate rocks, although the contact is not exposed. A smaller thrust sheet of similar meta-carbonate rocks overlies the succession.

The interbedded sandstones contain abundant grains of marble, metamorphic quartz and schist, together with abundant serpentinite, aphyric basalt, pyroxene-phyric basalt (relatively fresh and altered), dolerite (commonly altered), radiolarite (variably recrystallized), green and (rarely) blue chloritic grains, rare

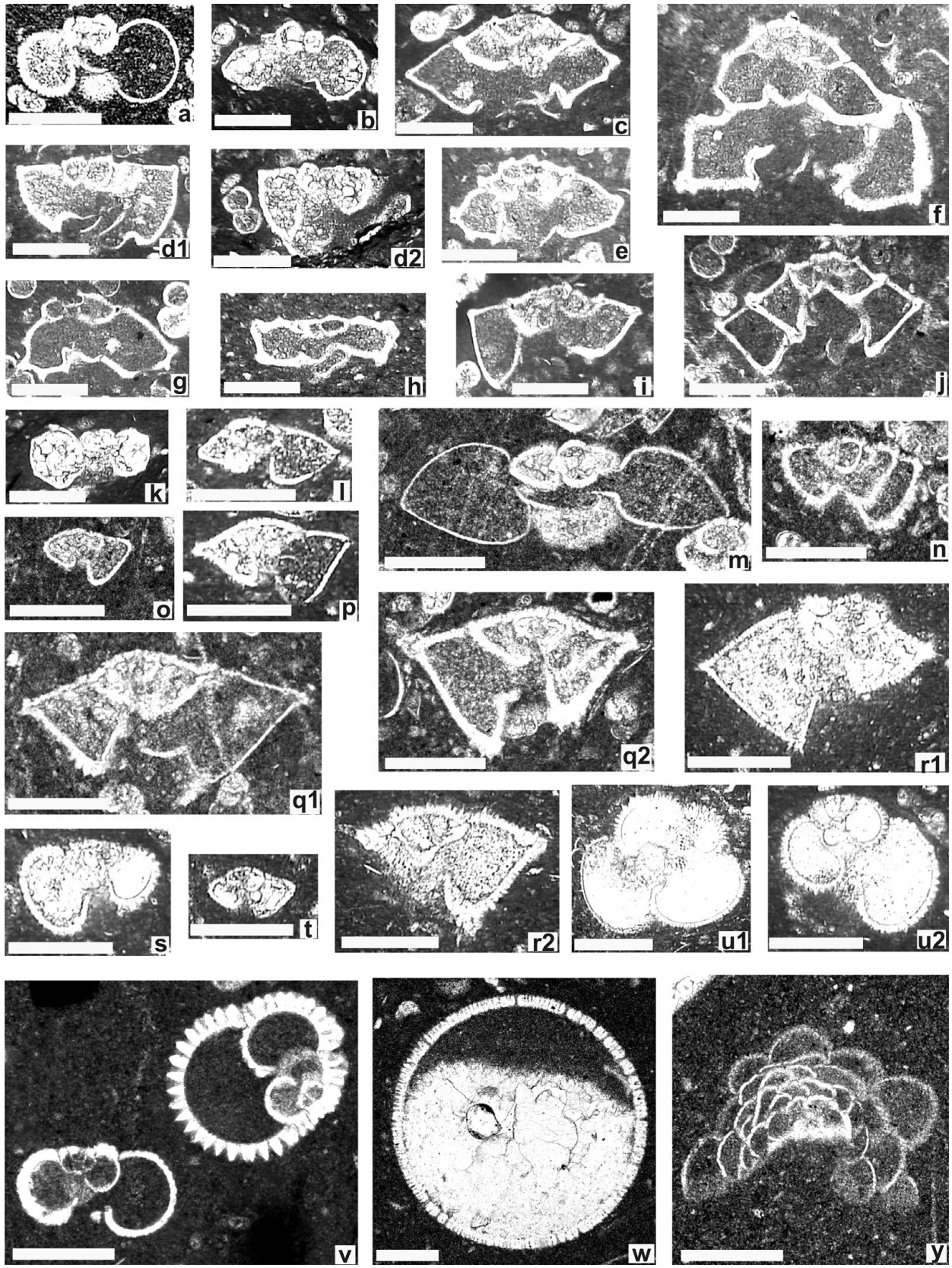

Figure 6. Photomicrographs illustrating key age-diagnostic foraminifera from the Kyrenia Range. (a) *Rugoglobigerina* sp., sample 06/21b; (b) *Rugoglobigerina scotti* (Brönnimann), sample 06/2a; (c) *Globotruncana falsostuarti* Sigal, sample 06/11a; (d1, d2) *Gansserina gansseri* (Bolli), samples 06/11d, 3a; (e) *Contusotruncana fornicata* (Plummer), sample 06/11d; (f, g) *Contusotruncana contusa* (Cushman), samples 06/10a, 11a; (h) *Abatomphalus mayaroensis* (Bolli), sample 06/21b; (i) *Globotruncanita stuartiformis* (Dalbiez), sample 06/11d; (j) *Globotruncanita stuarti* (De Lapparent), sample 06/10a; (k) *Globotruncana* cf. *bulloides* Vogler, sample 06/2a; (l, m) *Globanomalina pseudomenardii* (Bolli), samples 06/9a, 09/39; (n) *Acarinina* sp., sample 09/39; (o) *Morozovella* sp., sample 09/39; (p) *Morozovella aequa* (Cushman & Renz), sample 06/9a; (q1, q2) *Morozovella velascoensis* (Cushman), samples 09/39, 09/24; (r1, r2) *Morozovella spinulosa* (Cushman), sample 06/9b; (s) *Acarinina bullbrooki* (Bolli), sample 06/9b; (t) *Morozovella* sp., sample 06/9b; (u1, u2) *Globigerinatheka* sp., sample 06/9b; (v) *Subbotina* sp. and *Globigerinoides* sp, sample 06/18b; (w) *Orbulina* sp., sample 09/23; (y) *Planorbulina* sp., sample 09/23. Scale bars: 0.2 mm.

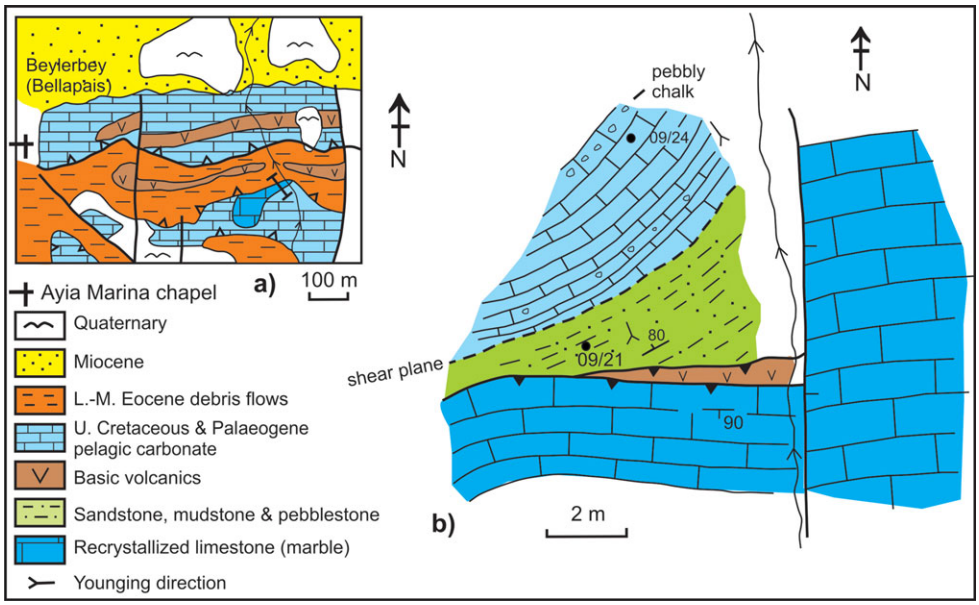

Figure 7. (Colour online) Field relations of several outcrops in the central Kyrenia Range that are correlated with the Maastrichtian Kiparisso Vouno (Alevkaya Tepe) Member; 1 km east of Ayia Marina chapel, near Beylerbey (Bellapais). (a) Outline geological map of the area south of Beylerbey (Bellapais), showing the location of the stream section studied in detail. (b) Local geological sketch map of the outcrop that matches the drawing and description of Baroz (1979). Steeply dipping, nearly massive marble (Trypa (Tripa) Gp) is in thrust-fault contact with a small wedge of very altered volcanic rocks, in turn followed by siliciclastic sediments. Fine- to medium-grained sandstones at the base are overlain by fine- to medium-grained, medium-bedded micaceous sandstone (1.8 m); medium-bedded coarse sandstone (0.6 m), well-cemented massive, pebbly sandstone (1.7 m), with well-rounded pebbles of red chert, basalt and marble (< 1 cm in size), and finally by medium–coarse-grained sandstone. A 10 cm break in exposure masks a shear plane, followed by relatively deformed but well-bedded pink chalk with scattered angular clasts of altered lava and some chert (0.3 m in size). Near the base the pelagic chalk contains a thin bed (< 5 cm) of breccia/conglomerate with marble clasts, up to 1.5 cm in size.

volcanic glass (hyaloclastite), plagioclase (relatively unaltered and altered), alkali feldspar (relatively altered) and pyroxene. Fragments of shell-rich micrite, large bivalve shells, polyzoan fragments, benthic foraminifera and rare planktonic foraminifera are also present (see online Appendix at http://journals.cambridge.org/geo). Three samples of calcareous sandstone (see Table 1) yielded reworked planktonic foraminifera of generally Late Cretaceous age (09/21), or a more precise Late Campanian–Maastrichtian age (samples 09/18 & 09/19).

The sandstone turbidites from the two outcrops in the Beylerbey (Bellapais) area (Fig. 7; Area 6 in Fig. 1) differ from the type area of the Kiparisso Vouno (Alevkaya Tepe) Member further west mainly owing to the presence of abundant ophiolite-related material (e.g. chert, basalt, serpentinite). There is little evidence that ophiolitic rocks were emplaced in the Kyrenia Range during Late Cretaceous time. However, possible source areas include ophiolitic rocks exposed in the Tauride Mountains to the north or potentially beneath the intervening Cilicia Basin (Okay & Özgül, 1984; Robertson, 1993; Kelling *et al*. 1987; Robertson *et al*. 2004).

4. Upper Cretaceous silicic and basaltic volcanic rocks

Following early mapping by Moore (1960), Baroz (1979, 1980) reported two contrasting magmatic assemblages that are best exposed in the western part of the Kyrenia Range. The first sequence, of inferred Upper Cretaceous ('Maastrichtian') age, was described as mainly basalt, dolerite, trachybasalt, trachyandesite, dacite and rhyolitic tuff. The second volcanic assemblage, of inferred Paleocene age, was mainly olivine basalt, trachyte and rare lamprophyre. Baroz (1980) interpreted the Upper Cretaceous igneous rocks as a calc-alkaline suite based on major element chemistry. Moore (1960) and Baroz (1979, 1980) also reported the existence of minor intrusions of several different lithologies.

Two contrasting volcanic suites are recognized here: first, a lower silicic sequence and secondly, a structurally overlying basaltic sequence; the latter is interbedded with pelagic carbonates of both Upper Cretaceous and Palaeogene age.

4.a. Silicic volcanogenic sequence

Sizeable areas of the western Kyrenia Range are characterized by silicic tuffaceous rocks and rhyolitic lava flows (termed the Yıldıztepe Volcanics by Hakyemez *et al*. 2000). These volcanic rocks are well exposed in the Geçiköy (Panagra) area (Area 2 in Fig. 1; Fig. 8) and the Selvilitepe (Fourkovouno) area (Area 3 in Fig. 1; Fig. 9), and are also known in a separate outcrop further west near Kayalar (Orga) (Area 1 in Fig 1; Fig. 10). Tiny outcrops of siliceous volcanics have also been mapped further east (e.g. NE of Aşağı Dikmen

Table 2. Summary of the main Cenozoic species of planktonic and benthic foraminifera identified during this study, utilizing the biozonation scheme of Sartorio & Venturini (1988)

SAMPLE NUMBER*	CHRONOSTRATI-GRAPHY	*Morozovella velascoensis* (Cushman)	*Morozovella aequa* (Cushman & Renz)	*Globanomalina pseudomenardii* (Bolli)	*Acarinina bullbrooki* (Bolli)	*Acarinina* sp.	*Morozovella spinulosa* (Cushman)	*Globigerinatheka* sp.	*Orbulina* sp.	*Globigerinoides* sp.	*Subbotina* sp.	*Mississippina* sp.	*Miscellanea* sp.	*Planorbulina* sp.
06/5a	UPPER PALEOCENE	X		X								X		
06/5b		X		X										
06/5c		X		X								X	X	
06/9a		X	Fig.6p	Fig.6l										
09/24		Fig.6q2	X	X		X								
09/39		Fig.6q1		Fig.6m		Fig.6n								
06/9b	MIDDLE EOCENE				Fig.6s		Fig.6r1, r2	Fig.6u1,u2						
09/30					X		X	X						
06/18a	MIDDLE MIOCENE TO HOLOCENE								X	X				
06/18b									X	Fig.6v	Fig.6v			
09/23									Fig.6w	X				Fig.6y

*See Appendix Table A2 for location data.

(Kato Dikomon)) between thrust sheets of marble (Baroz, 1979). Small exposures of silicic volcanic rocks are also seen between Upper Cretaceous pelagic limestones in the eastern Kyrenia Range (N of Ergenekon (Ayios Chariton)).

4.a.1. Type area of silicic volcanics

Despite local faulting and folding, exposures of silicic volcanic rocks are sufficiently continuous to suggest the existence of a single volcanic sequence in the western range. Baroz (1979) mapped this area as a southward-verging recumbent nappe (see Fig. 8a). Detailed remapping during this work, combined with the use of way-up criteria (e.g. local grading in tuffaceous sediments), enabled a stratigraphic sequence to be recognized, for example on the hillside east of Geçiköy (Panagra) gorge (Fig. 8a, g).

The silicic volcanic sequence exposed adjacent to Geçiköy (Panagra) gorge (Fig. 8a–b) and further east around Selvilitepe (Fourkovouno) (Fig. 9a) comprises two intergradational units. A lower interval of pale siliceous tuff (Fig. 8b) and rhyolitic debris flows (Fig. 4d) is followed by an upper interval dominated by thickly layered or massive rhyolitic lava flows (Fig. 9b, c).

The lower tuffaceous unit ranges from thin, to medium, to thick bedded, and from fine, to medium, to very coarse grained. The tuff is crudely stratified, locally forming weakly graded units. Numerous angular blocks of rhyolite, up to several metres in size, are entrained within coarse tuff. Thinner bedded, finer grained tuffaceous intercalations are commonly recrystallized to form dark grey flint. Thin-sections of the tuff exhibit angular fragments of isotropic silicic glass (Fig. 4e) with phenocrysts of quartz, plagioclase and biotite, also occasional entrained grains of fine-grained siliceous tuff or rhyolite. The higher part of the sequence is dominated by laterally discontinuous silicic lava flows, each up to $\sim$ 5 m thick.

The highest stratigraphically intact levels of the silicic sequence, exposed near the summit of Selvilitepe (Fourkovouno, F in Fig. 9a), are predominantly fine-grained silicic tuff (Fig. 9b, c). There is also a prominent bed of pale micritic carbonate (Fig. 9c) from which Baroz (1979) reported Late Cretaceous *Globotruncana* sp. This bed was relocated and sampled but was found to contain only very poorly preserved, non-identifiable planktonic foraminifera. Two samples of siliceous tuff from the Geçiköy (Panagra gorge) and Selvilitepe (Fourkovouno) outcrops have been dated using the whole-rock Ar–Ar method, yielding a Campanian age (K. Huang, unpub. M.Sc. thesis, Univ. Hong Kong, 2008).

The silicic volcanogenic succession is cut by small basaltic intrusions in several areas (e.g. Fig. 9b, c). Although mapped by Baroz (1979) as alkaline lava flows within silicic volcanogenic rocks, they map out as irregular, cross-cutting intrusions bounded by chilled margins. These bodies exhibit reaction zones up to

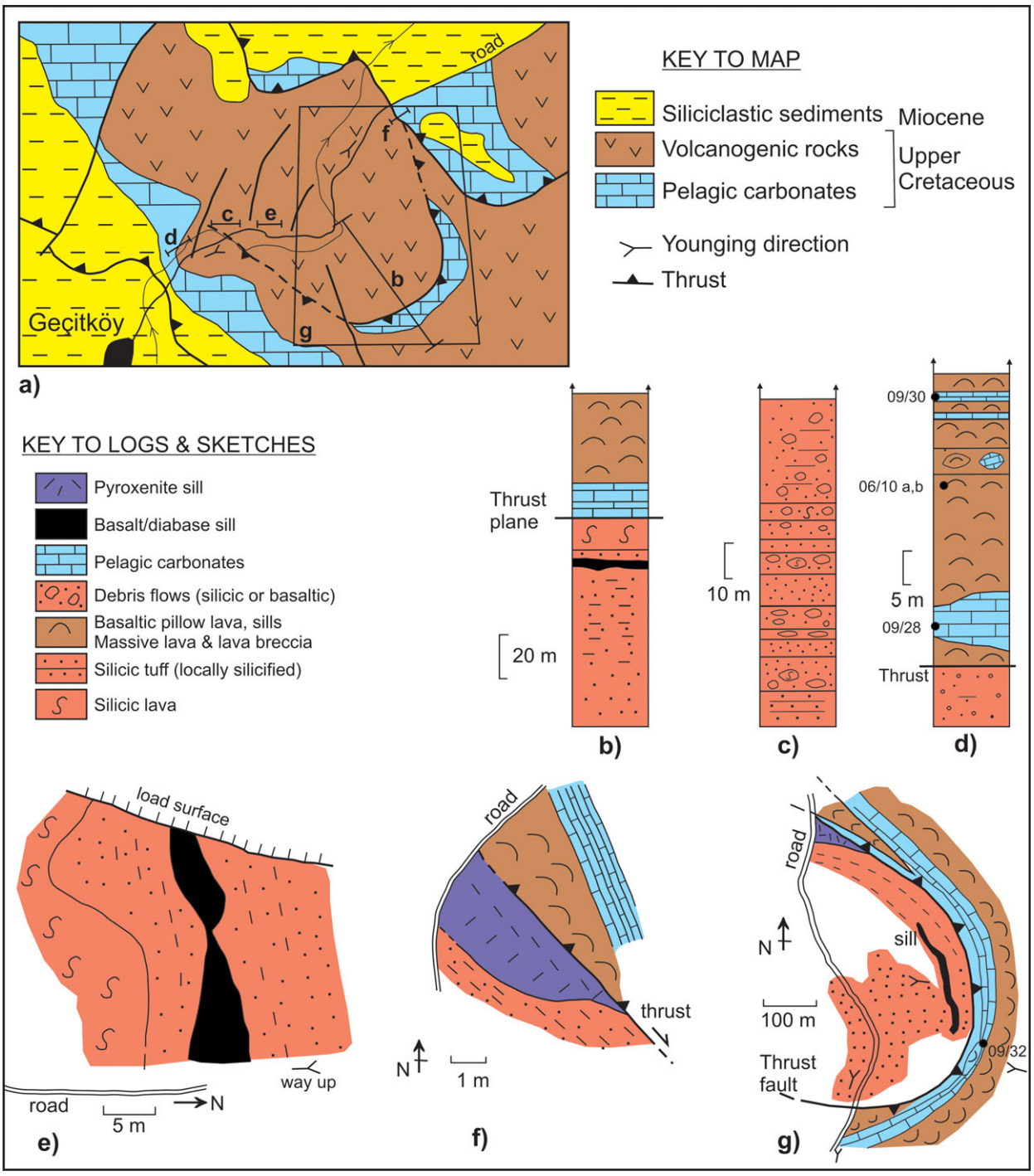

Figure 8. (Colour online) Field relations of Upper Cretaceous volcanic and sedimentary rocks exposed near Geçiköy (Panagra) in the western Kyrenia Range (Area 2 in Fig. 1). (a) Outline geological map based on Baroz (1979), Moore (1960) and this work. The area is dominated by a recumbent SE-verging anticline of inferred Late Miocene–earliest Pliocene age. (b) Measured log of the section marked b on the map in (a). The lower part comprises well-bedded tuff with coarser and finer interbeds (< 0.5 m thick) and rare tuffaceous debris flows (clasts < 2 cm in size). The thrust plane is characterized by small duplexes of basalt entrained along the contact. (c) Local log of part of the silicic volcanogenic sequence exposed along the main road. This begins with a volcanic conglomerate with mainly sub-rounded to sub-angular boulders of hard flinty rhyolite in a pale, chaotic debris-flow unit. The sequence grades upwards into relatively massive white tuff with scatted small lava clasts. Overlying thick debris flows include angular clasts of grey flinty rhyolite clasts (up to 2.5 m in size). Interbedded fine-grained tuff contains scattered rhyolite blocks (up to 0.8 m in size). (d) Local log of basalt and pelagic chalk sequence exposed in the road section, structurally above the silicic volcanogenic sequence (see (c)). The chalk is interbedded with pillow basalt, lava breccia and hyaloclastite mixed with chalk. Chalk interbeds are dated as Late Campanian–Maastrichtian (sample 09/28) and as Late Maastrichtian (sample 06/10a, b), while pelagic limestone interbedded with pillow basalt along the road section to the south is dated as Middle Eocene (sample 09/30). (e) Part of the sequence along the north side of the main road exposes weakly bedded silicic tuff, locally overlain by a vitreous rhyolite flow. A small irregular body interpreted as a high-level basaltic intrusion cuts the tuff. (f) Pyroxenite sill intruding tuffaceous sediments. The intrusion is truncated by a thrust, above which comes a contrasting succession of Upper Cretaceous pelagic chalk and basalt. (g) The lower silicic lava/tuff sequence and the overlying Upper Cretaceous pelagic chalk/basalt sequence are separated by a thrust. Both sequences are folded into a SE-facing anticline of Late Miocene–earliest Pliocene age.

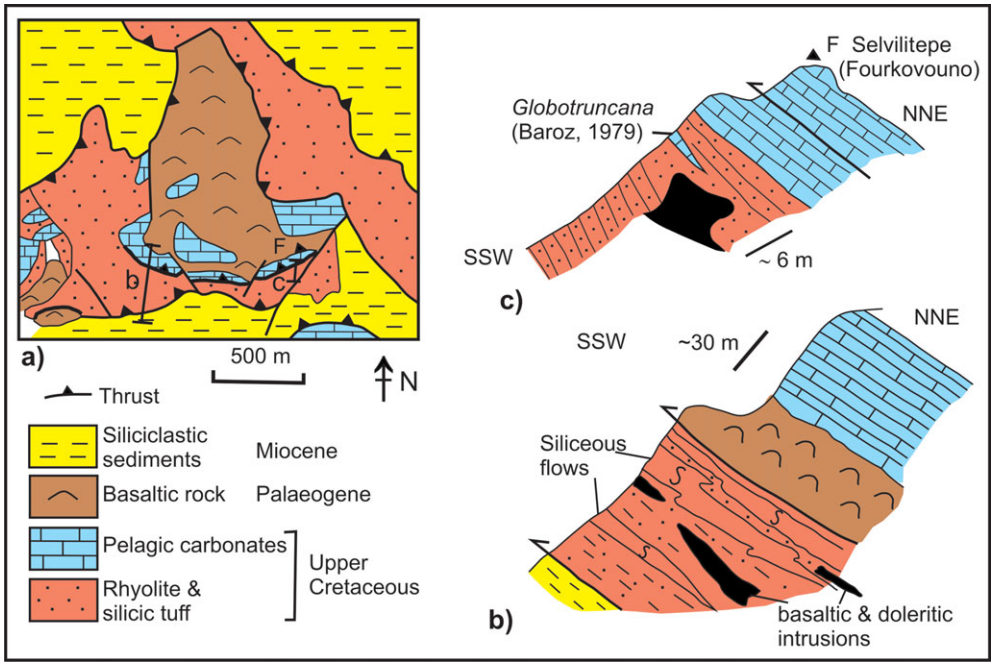

Figure 9. (Colour online) Field relations of the Upper Cretaceous volcanic and sedimentary rocks exposed near Selvilitepe (Fourkovouno) to the east of Geçiköy (Panagra); Area 3 in Figure 1. (a) Outline geological map, modified from Baroz (1979). A thrust separates silicic tuff and rhyolite below from a pillow basalt–pelagic chalk sequence above. Pillow lava and pillow breccia in the southwest of the area mapped appear to be stratigraphically inverted owing to the presence of a S-facing recumbent fold (see Fig. 8g). (b) Local profile showing the lower sequence of silicic tuffs and lenticular rhyolitic flows that are interbedded with silicic tuffs and cut by elongate sill-like basaltic intrusions. Upper Cretaceous basaltic pillow lavas and pelagic carbonates as exposed structurally above this. (c) Highest exposed part of the silicic volcanogenic rocks, overlain by silicic tuff and tuffaceous chalk, followed above a thrust plane by Upper Cretaceous pelagic chalk (pillow basalt is exposed further north). The uppermost silicic tuff beneath the thrust is brecciated, while overlying chalk just above the thrust is sheared. The thrust cuts obliquely across the tectonostratigraphy at a low angle (< 25°).

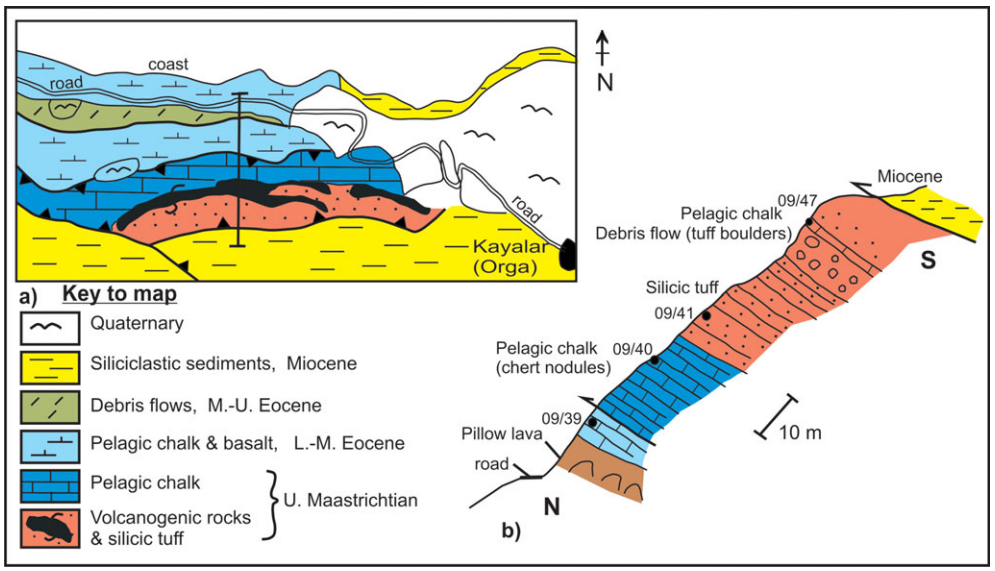

Figure 10. (Colour online) Field relations of volcanogenic rocks and pelagic carbonates exposed west of Kayalar (Orga) in the most westerly part of the western Kyrenia Range (location 1 in Fig. 1). (a) Geological sketch map based on Moore (1960), Baroz (1979) and this study. Exposure is limited on a bush-covered hillside south of the road. Basalts are interbedded with Paleocene chalk in the north (near the road) while pelagic chalk interbedded with silicic tuff higher on the hillside (southwards) is dated as Late Cretaceous, confirming the existence of the mapped thrust. (b) Profile showing the upward passage from Upper Cretaceous pelagic chalk, to silicic tuff and then into coarser volcanogenic debris flows interbedded with Upper Cretaceous pelagic chalk.

several metres thick in contact with silicic host rocks. Tuff in close vicinity (< 5 m) to the intrusions is recrystallized to hard, dark grey, flinty silicic rock. Thin-sections of the small intrusions reveal classic doleritic textures with intersertal plagioclase, augite and opaque grains set within interstitial glass. The basaltic intrusions are here interpreted as high-level intrusions into soft, wet, poorly consolidated siliceous tuffaceous sediments.

The contact between the siliceous volcanogenic rocks and the overlying basaltic lavas (with interbedded pelagic carbonates) is interpreted as a low-angle tectonic contact, probably a thrust. The contact is well exposed on the eastern side of the main road through Geçiköy (Panagra) gorge (Fig. 8a, f), on the hillside to the east (marked on section b in Fig. 8a), and also near the summit of Selvilitepe (Fourkovouno) (Fig. 9c).

4.a.2. Silicic sequence in a more westerly comparative area

Additional exposures exist further west, in the Kayalar (Orga) area (Fig. 10). Lavas and pelagic carbonates are exposed along the coastal road section and on the brushy hillside above (Fig. 10a). A thin-section of chalk from near the base of the hillside (Fig. 10b) revealed planktonic foraminifera of Late Paleocene age (sample 09/39; Fig. 6q1, m, n; Table 2). Above a non-exposed interval (~ 5 m), two other samples of chalk contain well-preserved planktonic foraminifera of Late Maastrichtian age (samples 09/40 & 09/41; Table 1). Sedimentary structures (e.g. grading) show that the succession is stratigraphically the right way up. A thrust fault is, therefore, inferred between the dated Palaeogene and Maastrichtian intervals (Fig. 10b). Pelagic lavas and interbedded basaltic pillow lavas below the thrust are correlated with the Palaeogene Ayios Nikolaos (Yamaçköy) Formation of the Lapithos (Lapta) Group.

Above the inferred thrust fault the colour changes from pink to grey, and the lithology from thin- to medium-bedded pelagic carbonate, to fine-to medium-grained, well-bedded siliceous tuff. The bedding in the pelagic carbonates below and above the lowest tuff occurrence is conformable, without evidence of a tectonic contact between these two lithologies (Fig. 10b). A thin-section of the typical tuff revealed a glassy fragmental texture (hyaloclastite), with mainly fragmented phenocrysts of quartz, plagioclase and biotite.

Upwards over ~ 10 m the tuffaceous sediments become gradually coarser, culminating in coarse silicic tuff and rhyolitic lava flows, similar to those exposed further east in the Geçiköy (Panagra) area (see previous Section). The rhyolite comprises phenocrysts of quartz, biotite and plagioclase (partially calcite replaced) set in a glassy silicic matrix with small opaque grains. Higher levels of the coarse tuff show evidence of reworking and the sequence then passes into a prominent horizon of heterogeneous breccia/conglomerate (several metres thick) with sub-angular to angular clasts of basalt, subordinate coarse silicic tuff (clasts up to 30 cm in size; Fig. 4f). This unit is depositionally overlain by pink pelagic carbonate, rich in detrital grains of the same composition as in the underlying breccia-conglomerate. This chalk contains well-preserved Late Maastrichtian planktonic foraminifera (sample 09/47; Table 1). Further tuffaceous sediments are poorly exposed on the hillside above but not as a coherent succession.

In summary, the restored Upper Cretaceous sequence in this area begins with pelagic carbonate (with no known base) and passes upwards into a thickening- and coarsening-upward sequence of water-lain siliceous tuff and subaqueous mass flows, and culminates in thick-bedded to massive silicic lava flows. The overlying conglomerate with both siliceous and basaltic clasts shows that both of these lava compositions were exposed in the area and were reworked in a deep-sea setting during Late Maastrichtian time.

4.a.3. Basaltic-pelagic carbonate unit

Basaltic lavas (Çınarlı Volkanics of Hakyemez *et al*. 2000) overlie the basal unconformity of the Upper Maastrichtian Melounda (Mallıdağ) Formation in several areas of the western Kyrenia Range. For example, near Karşıyaka (Vassileia) the basal carbonate breccias are overlain by several metres of pelagic chalk rich in Late Maastrichtian planktonic foraminifera, as noted above (see Fig. 6c, d, e, i; Table 1). Interbedded basaltic lavas, lava breccia and pink pelagic carbonates follow above this (Fig. 3c). The lower part of the volcanic succession includes several intercalations of lenticular carbonate breccia (up to 0.6 m thick), dominated by angular marble clasts derived from the Mesozoic meta-carbonate platform.

Alternations of pelagic carbonates and basaltic rocks are also well exposed in the southern part of Geçiköy (Panagra) gorge, along the hillsides on both sides of the main road (Fig. 8a, d) and also further west in the Selvilitepe (Fourkovouno) area (Fig. 9). One sample (09/28) of pelagic chalk from the lower part of the basaltic succession in Geçiköy (Panagra) gorge (to the west of the main road; Fig. 8d) was dated as Late Campanian–Maastrichtian (see Table 1). Two further samples (06/10a, b) from higher in the same sequence (also on the western side of the road) yielded a Late Maastrichtian age (see Table 1). One sample of pelagic chalk from just above the exposed base of the basaltic sequence on the hillside east of Geçiköy (Panagra) gorge was dated as Late Campanian–Maastrichtian (sample 09/32; see Table 1). In contrast, another sample of pelagic chalk interbedded with basaltic lava higher in a southward-younging sequence (along the eastern side of the main road; Fig. 8d) was dated as Middle Eocene (Fig. 6r1, r2, u1, u2; Table 2). Several samples of basaltic lavas from the Geçiköy (Panagra) road section have been dated by the Ar–Ar whole-rock method at ~ 50 Ma age (Early Eocene) (K. Huang, unpub. M.Sc. thesis, Univ. Hong Kong, 2008). However, the exact

position of these samples with respect to our dated pelagic chalks is unclear.

4.b. Basic volcanic rocks elsewhere in the Kyrenia Range

Pelagic chalks were collected and dated from lava–sediment associations throughout the eastern part of the central Kyrenia Range, the eastern Range and the Karpas Peninsula (Fig. 1). Samples have also been collected from many of these outcrops for palaeomagnetic study, mainly to shed light on any tectonic rotations that could have affected the Kyrenia Range (Hodgson *et al*. 2010). The basaltic extrusive rocks are most extensive in the eastern range, where they have been interpreted as intercalations within the Upper Cretaceous Melounda (Mallıdağ) Formation and the Palaeogene (Ayios Nikolaos (Yamaçköy) Formation) (Baroz, 1979; Robertson & Woodcock, 1986; Hakyemez *et al*. 2000; Fig. 2).

Pelagic carbonate within the interstices of pillow lavas exposed in a quarry ∼ 1 km west of Değirmenlik (Kithrea) (Fig. 11a) yielded a Late Maastrichtian age (samples 06/28a–c; Table 1) and is, therefore, correlated with the Melounda (Mallıdağ) Formation. In addition, a sample of pelagic chalk interbedded with pillow lava was collected from a road section between Halevga (Halevka) and Değirmenlik (Kithrea) (sample 06/27a) and this also gave a Late Maastrichtian age (Table 1). Near Ergenekon (Agios Khariton), two samples of pelagic carbonate overlying a massive lava flow (Fig. 11b; samples 06/31a, b) provided Late Campanian–Maastrichtian and Late Maastrichtian ages, respectively (see Table 1). Near Tirmen (Trypimeni) two samples of pelagic chalk within stratigraphically inverted pillow basalts gave Late Maastrichtian ages (Fig. 11ci). One sample (06/3a; Fig. 6d2; Table 1) was collected from pelagic limestone mixed with volcanic detritus from just beneath a basaltic lava flow; another (06/4a) came from a lens of pelagic limestone between pillow lava. Several other samples were collected higher in the succession in this area, 1.5 km NNW of Tirmen (Trypimeni). These are associated with a thick lava flow (∼ 60 m) that is underlain by red siliceous shale, pelagic carbonate and fine-grained calciturbidites. The pelagic carbonate was dated as Late Paleocene (Fig. 11cii; Table 2).

Pelagic chalk interbedded with basaltic lava flows further east near Çınarlı (Platani) (Fig. 11di) yielded a Late Maastrichtian age (sample 06/8a; Table 1). Higher in the succession in this area (0.5 km further west; Fig. 11dii), pelagic chalk interbedded with massive lava flows (sample 06/9a) furnished a Late Paleocene age, while a sample higher in the sequence (06/9b) was dated as Middle Eocene (Fig. 6l, p; Table 2). Near Mallıdağ (Melounda) (Fig. 11e) one sample of grey pelagic chalk interbedded with massive lava (sample 06/1a) yielded a Late Campanian–Maastrichtian age, while another (sample 06/2a) gave a Late Maastrichtian age (Fig. 6b). Pelagic limestone interbedded with lava flows near Ağıllar (Mandres) village (Fig. 11f) was dated as Late Campanian–Maastrichtian (sample 06/29a) and Late Maastrichtian (sample 06/29b). Pelagic limestone interbedded with pillowed flows from a road section 1.75 km east of Ağıllar (Mandres) (sample 06/30) also gave a Late Maastrichtian age (see Table 1).

In addition, pelagic chalk was also collected from a large exposure (∼ 7 km E–W × 2.5 km N–S) of thrust sheets dominated by pillow basalt near Balalan (Platanisso) in the Karpas Peninsula (Fig. 11g; see G. McCay, unpub. Ph.D. thesis, Univ. Edinburgh, 2010). Pinkish interpillow carbonate is commonly present in several different thrust sheets. Pelagic carbonate also fills in numerous sub-vertical neptunian fissures that transect the lavas. Interpillow pelagic carbonate (∼ 80 m NNW of Balalan mosque; Fig. 11gi) is dated as Late Maastrichtian (samples 06/17a–e; Table 1). Pelagic carbonate filling nearby neptunian fissures (samples 06/18a, b & GM09/23) was dated only generally as Miocene–Holocene based on planktonic foraminifera including *Orbulina* sp. and *Globigerinoides* sp. (Fig. 6v, w, y; Fig. 11gii). In another outcrop ∼ 400 m SSW of Balalan (Fig. 11giii) three samples were collected from a small lens of pelagic carbonate within pillow lava (5 m × 1 m thick), mixed with pillow lava debris. These three samples (06/21a–c) were dated as Late Maastrichtian (Fig. 6a, h; Table 1). Two samples of interstitial pelagic chalk (e.g. sample 06/26a) from a separate thrust sheet of pillow lava further north, along the northern edge of the Balalan outcrop (Fig. 11giv), yielded a general Late Cretaceous age (see Table 1).

In summary, the new age data (Fig. 12) indicate that the basaltic lavas within the Melounda (Mallıdağ) Formation are mainly Late Maastrichtian in age. In contrast, the basalts associated with the overlying Ayios Nikolaos (Yamaçköy) Formation range from Late Paleocene to Middle Eocene.

5. Discussion and interpretation

5.a. Metamorphism and exhumation of the Mesozoic carbonate platform

The tectonic development of the Kyrenia Range during Late Cretaceous time can be related to northward subduction of the Southern Neotethys beneath Tauride continental units, stretching from the Eastern Mediterranean (Robertson & Woodcock, 1986; Robertson, 1998) eastwards through eastern Anatolia to Iran (Aktaş & Robertson, 1984, 1990; Yılmaz, 1993; Fig. 13). In this interpretation it should be noted that the Troodos ophiolite, the Hatay ophiolite (e.g. Parlak *et al*. 2004) and the Baer-Bassit ophiolite (e.g. Al-Riyami *et al*. 2002), amongst others formed at ∼ 90 Ma above a separate more southerly intra-oceanic subduction zone (e.g. see Musaka & Ludden, 1987; Moores & Vine, 1971; Gass, 1990; Robinson & Malpas, 1990; Robertson & Xenophontos, 1993).

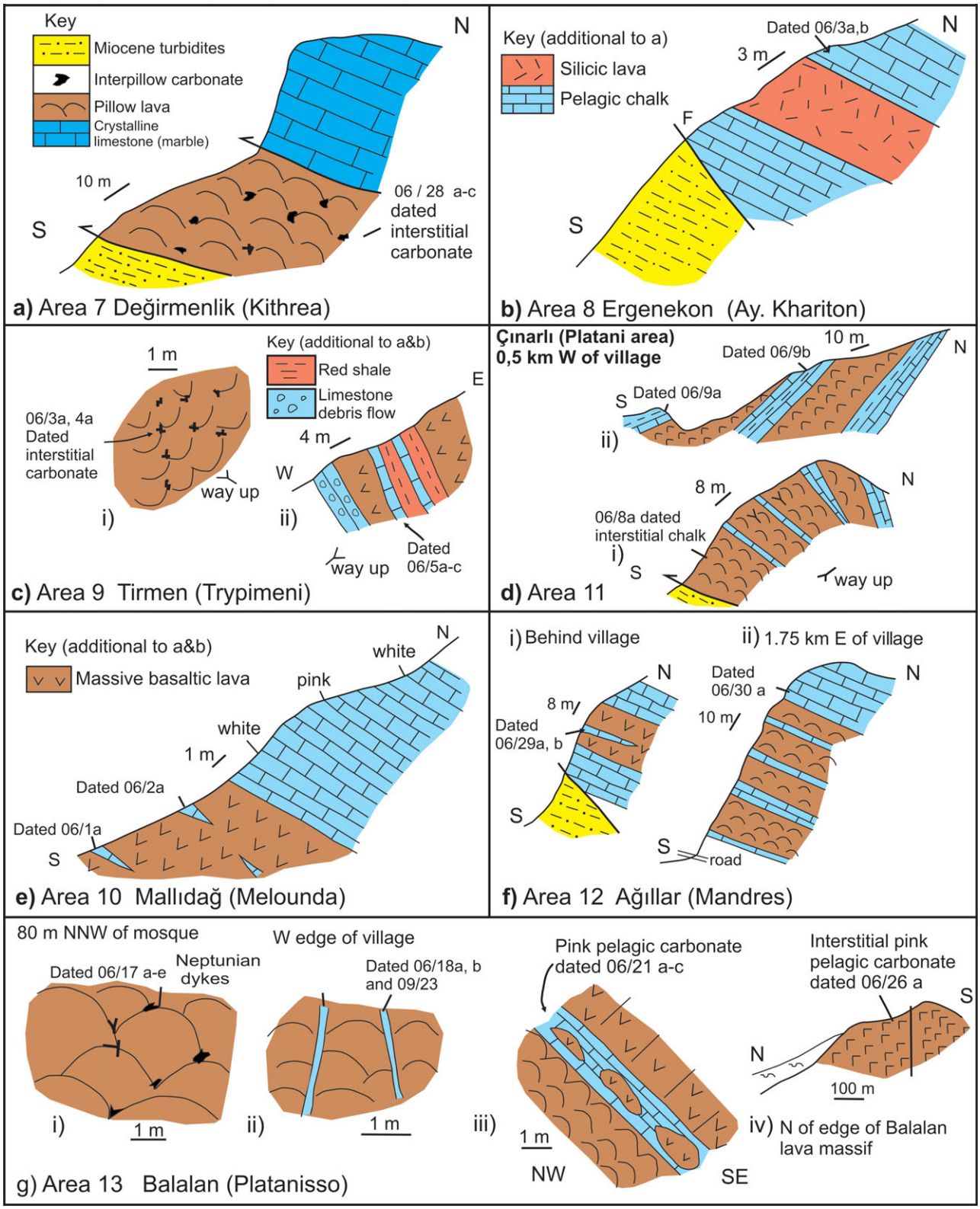

Figure 11. (Colour online) Field relations of dated chalks associated with basaltic lavas in the central and eastern Kyrenia Range, areas 7–13. See text for an explanation of each area. The locations of samples are listed in Tables A1 and A2.

The Mesozoic carbonate platform is interpreted as part of a microcontinent that rifted from Gondwana during spreading of the Southern Neotethys, beginning in the Late Triassic. The ocean began to close related to northward subduction during Late Cretaceous time.

There are two main alternatives to explain the greenschist-facies metamorphism of the Kyrenia platform prior to Late Maastrichtian time (Fig. 13). First, the Kyrenia platform rifted in Triassic time to form a small continental fragment with a larger Tauride microcontinent to the north (Fig. 13a; Alternative 1).

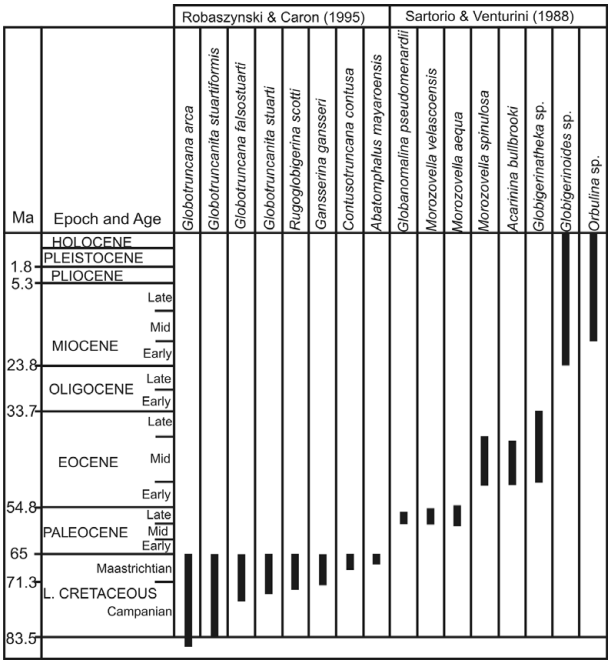

Figure 12. Summary of the ranges of some of the age-diagnostic planktonic foraminifera identified from thin-sections during this work, associated with various volcanogenic lithologies throughout the Kyrenia Range. The main source references are indicated. The species age ranges suggest that the volcanism mainly occurred during Late Maastrichtian and Late Paleocene time. A Mid-Eocene age was recognized at only one locality. The Neogene–Recent age refers to planktonic foraminifera that were reworked into neptunian fissures and do not indicate a time of volcanism.

Northward subduction culminated in collision of two rifted microcontinents and as a result the Kyrenia platform was buried to at least several kilometres depth, converting carbonate rocks to marble, and subordinate argillaceous rocks to pelite and micaceous schist. There is, however, no known evidence of high-pressure/low-temperature metamorphism affecting the Kyrenia Range, suggesting that complete subduction did not take place. In the second alternative the Kyrenia platform formed part of a larger continent including the Tauride carbonate platform to the north, as exposed north of Cyprus (Okay, 1989; Okay & Özgül, 1984; Robertson, 1993; Fig. 13 Alternative 2). In this case the southward edge of the regional-scale platform was somehow detached and thrust beneath a larger continental unit to the north, resulting in burial metamorphism. Such detachment might have nucleated along an intra-platform rift, if present. More work is necessary, especially on the metamorphic rocks of the Alanya Massif to the north of Cyprus (Okay, 1989) to help distinguish between the two alternatives. However, the first alternative involving subduction and the collision of two carbonate platforms seems more plausible.

In both alternatives the buried Kyrenia platform was soon exhumed, perhaps owing to the buoyancy of continental crust, or subduction-related slab rollback (see Fig. 13a, b). The widespread jigsaw-type breccias in the meta-carbonate rocks could relate to extensional exhumation of the Mesozoic carbonate platform.

The tectonic exhumation of the Kyrenia meta-platform to the seafloor allowed an unconformity to develop that was soon covered by sedimentary breccias and pelagic carbonates. Fault controlled hollows in the seafloor were then filled in by calcareous sandy turbidites of the Kiparisso Vouno (Alevkaya Tepe) Member, mainly derived from a remote continental source. The Upper Cretaceous sandstone turbidites in the central Kyrenia Range (Beylerbey (Bellapais) area) were additionally derived from an ophiolitic source, presumably located further north.

5.b. Formation of the Upper Cretaceous and Palaeogene igneous rocks

Baroz (1979, 1980) interpreted the Upper Cretaceous volcanic rocks as a calc-alkaline assemblage that erupted following closure of the Tethys in this region. The eruption of Palaeogene volcanic rocks reflected post-collisional transcurrent movement between Africa and Anatolia in his interpretation. However, the then-available whole-rock chemistry was inadequate to support a robust tectonic interpretation. A basalt sample from the central Kyrenia Range was later noted to exhibit the typical 'enriched' signature of within-plate basalt using immobile major- and trace-element tectonic discrimination (Pearce, 1975). Basaltic rocks were subsequently analysed by Robertson & Woodcock (1986) from both the Upper Cretaceous and Palaeogene sequences (34 samples) throughout the Kyrenia Range (including the Balalan (Platanisso) and Geçiköy (Panagra) areas) and were found to be mainly of alkaline, within-plate type. However, some samples showed relatively low MORB (mid-ocean ridge basalt)-normalized values of Nb, atypical of within-plate-type basalts.

Recently, Huang, Malpas & Xenophontos (2007) (see also K. Huang, unpub. M.Sc. thesis, Univ. Hong Kong, 2008) reported the results of high-quality major element, trace element and rare earth element (REE) analysis of basic and silicic volcanic rocks from the western, central and eastern Kyrenia Range. The silicic lavas of the western range (Geçiköy (Panagra) and Kayalar (Orga)) area were interpreted as volcanic arc basalts, strongly affected by crystal fractionation, comparable for example with the modern Andean continental margin arc. In contrast, basalts from the western range area are dissimilar to typical arc basalts but show affinities with 'transitional arc' to within-plate basalt. In addition, basalts from the central range (Mallıdağ (Melounda), Yamaçköy (Ayios Nikolaos) and Bahçeli (Kalograia)) are of enriched within-plate type, but with small negative Ce and Hf anomalies. The basalts from the eastern range and the Karpas Peninsula Çınarlı (Platani) and Balalan (Platanisso) are again of intra-plate type, but show lesser 'enrichment' relative to MORB (Huang, Malpas & Xenophontos, 2007; see

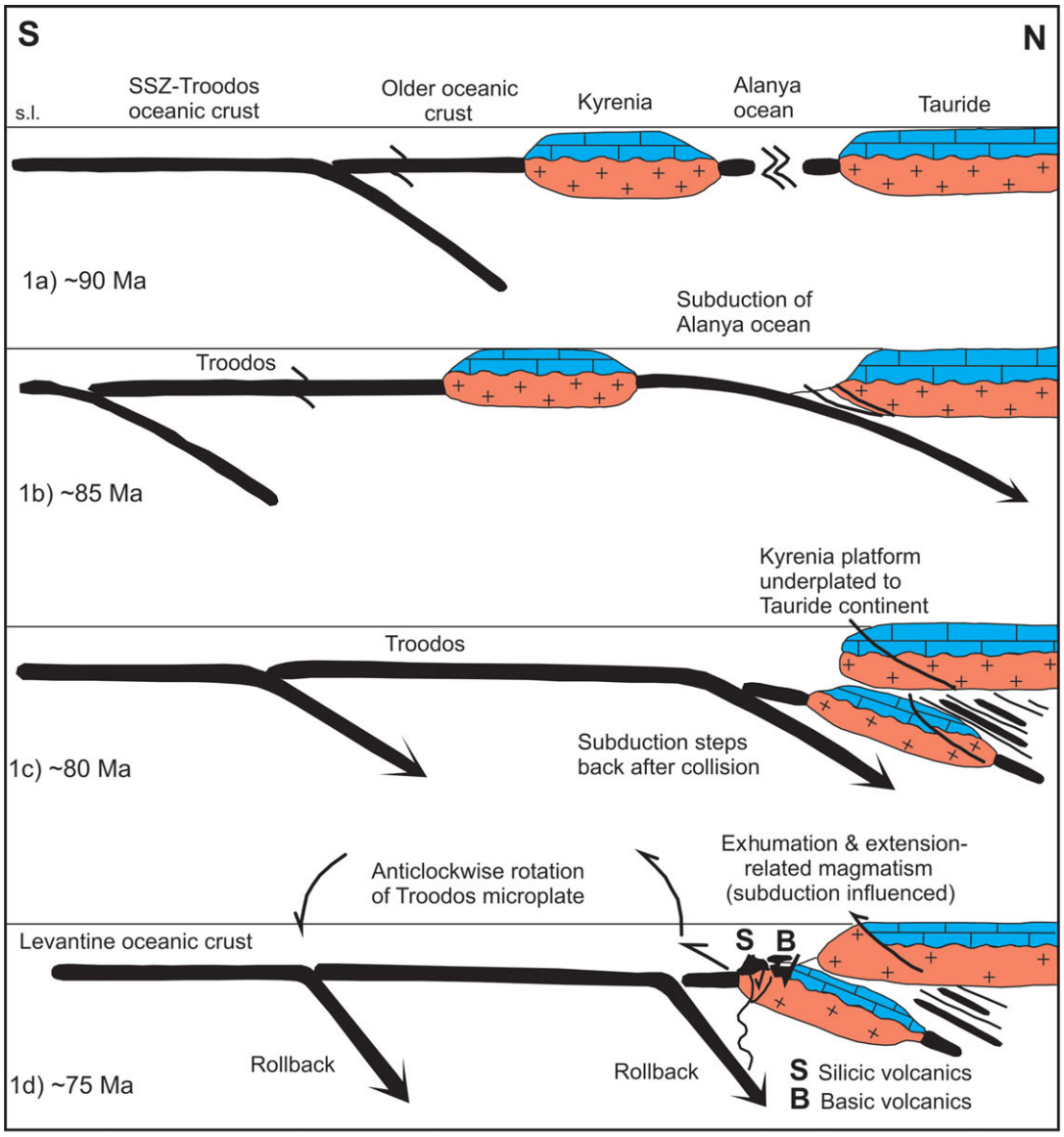

Figure 13. (Colour online) Plate tectonic interpretations of the Late Cretaceous tectonic development of the Kyrenia Range. Alternative 1. (1a) After spreading of oceanic lithosphere on either side of the Kyrenia platform, northward subduction initiated within the Southern Neotethys and the Troodos ophiolite formed to the south by supra-subduction zone (SSZ)-type spreading. The Mesozoic

also K. Huang, unpub. M.Sc. thesis, Univ. Hong Kong, 2008).

The silicic and basaltic sequences of the western range are separated by a tectonic contact, presumably a thrust (of unknown displacement). This opens the possibility that the two volcanic sequences erupted far apart (i.e. > tens of kilometres) but were later brought together by thrusting. If so, they could have erupted contemporaneously in different tectonic settings (e.g. arc versus back-arc basin). However, several factors suggest that the two lava sequences formed within a single area of volcanic activity.

First, the two volcanic sequences are not separated by Palaeogene or Neogene sediments in contrast to many of the major thrust sheets elsewhere in the Kyrenia Range (Baroz, 1979; Robertson & Woodcock, 1986). Secondly, the small intrusions of diabase within the silicic sequence are of typical alkaline within-plate type (Baroz, 1979, 1980). It is possible that these alkaline intrusions fed 'enriched' basalts at higher levels (Upper Cretaceous or Palaeogene) that are no longer exposed. Similar alkaline basalt lavas of Late Maastrichtian and Paleocene ages are present in the overlying sequence, although separated by a thrust plane. Thirdly, debris flows in the comparative, westerly Kayalar (Orga) area contain both basaltic and silicic volcanic debris showing that both lava compositions were exposed locally.

The lower volcanogenic sequence is restored as pelagic carbonates and silicic tuffs, coarsening upwards into silicic debris flows and then into massive rhyolite flows (Fig. 14a). The field relations suggest the construction of a substantial subaqueous volcanic edifice, perhaps several hundred metres high. The emplacement of the silicic volcanic debris flows is likely to have been triggered by periodical gravity collapse.

The Maastrichtian basaltic volcanics are observed to overlie an exhumed Mesozoic carbonate platform, whereas no basement to the silicic volcanics is exposed. However, the chemical composition of the silicic volcanics is suggestive of the former existence of a continental basement (see Huang, Malpas & Xenophontos, 2007; K. Huang, unpub. M.Sc. thesis, Univ. Hong Kong, 2008).

Two alternative tectonic settings for the Upper Maastrichtian and also the Upper Paleocene–Middle Eocene basaltic volcanic rocks can be considered. Many of the basalts from the western, central and eastern Kyrenia Range, but apparently not from the Karpas Peninsula (e.g. Balalan (Platanisso)), show evidence of negative Nb and Hf anomalies relative to typical within-plate basalts (Robertson & Woodcock, 1986; Huang, Malpas & Xenophontos, 2007; see also K. Huang, unpub. M.Sc. thesis, Univ. Hong Kong, 2008). This could be interpreted to indicate contemporaneous Late Maastrichtian and also Late Paleocene–Middle Eocene subduction. Alternatively, the subduction chemical signature (in either or both of the volcanic episodes) could have been inherited from subcontinental mantle lithosphere after subduction ceased in the area. This explanation is preferred here in the absence of other evidence of coeval Late Maastrichtian or Late Paleocene–Middle Eocene subduction (e.g. calc-alkaline magmatism; tuffaceous sediments) (Figs 13, 14).

5.c. Timing of deformation of the Upper Cretaceous and Palaeogene sequences

The timing of the deformation of the Upper Cretaceous–Palaeogene lava sequences (Fig. 14) is constrained by the tectonostratigraphy of the Kyrenia Range as a whole. There is no evidence that compressional deformation affected the Kyrenia Range between the time of development of the Upper Cretaceous unconformity and the regional Mid-Eocene thrusting that affected the range as a whole (Fig. 14b). Large-scale thrusting and folding also took place during Late Miocene time (Baroz, 1979; Robertson & Woodcock, 1986; Hakyemez *et al*. 2000; G. McCay, unpub. Ph.D. thesis, Univ. Edinburgh, 2010; Fig. 14c). In the western Kyrenia Range the sheared contact separating the silicic and basaltic sequences is deformed by the Late Miocene deformation phase. It is therefore likely that the silicic and basaltic sequences were first compressionally deformed during the regional Mid-Eocene southward thrusting event.

6. Comparison with adjacent regions

6.a. Comparable Late Cretaceous magmatism

The volcanogenic Kannaviou Formation in western Cyprus is comparable with the silicic volcanics exposed in the Kyrenia Range. This formation depositionally overlies the Upper Cretaceous pillow basalts of the

carbonate platform (Trypa (Tripa) Gp) is viewed as a Triassic-rifted continental fragment that was later re-amalgamated to a larger Tauride microcontinent to the north. (1b) Inferred oceanic crust between the Kyrenia platform and the Tauride continent was subducted northwards. (1c) The Kyrenia platform collided with the Tauride continent and was underthrust (underplated) resulting in regional greenschist-facies metamorphism. After collision the trench rolled back allowing the Kyrenia platform to rapidly exhume. (1d) With continuing subduction coupled with slab rollback, Campanian?–Maastrichtian silicic-arc-type volcanic rocks erupted, coupled with Maastrichtian basic volcanism further north. Slab rollback (potentially of two oceanic plates) accommodated anticlockwise rotation of the Troodos microplate beginning in Campanian time (see Fig. 15). Alternative 2. The Mesozoic carbonate platform (Trypa (Tripa) Gp) is viewed as the southern part of a larger Tauride microcontinent. (2a) The Southern Neotethys subducted beneath this combined microcontinent. (2b) The continent detached into upper and lower plates (perhaps failing along a Triassic rift) with the Kyrenia platform being thrust beneath the Tauride platform. The later development was similar to (1d). Alternative 1 is preferred. See text for discussion.

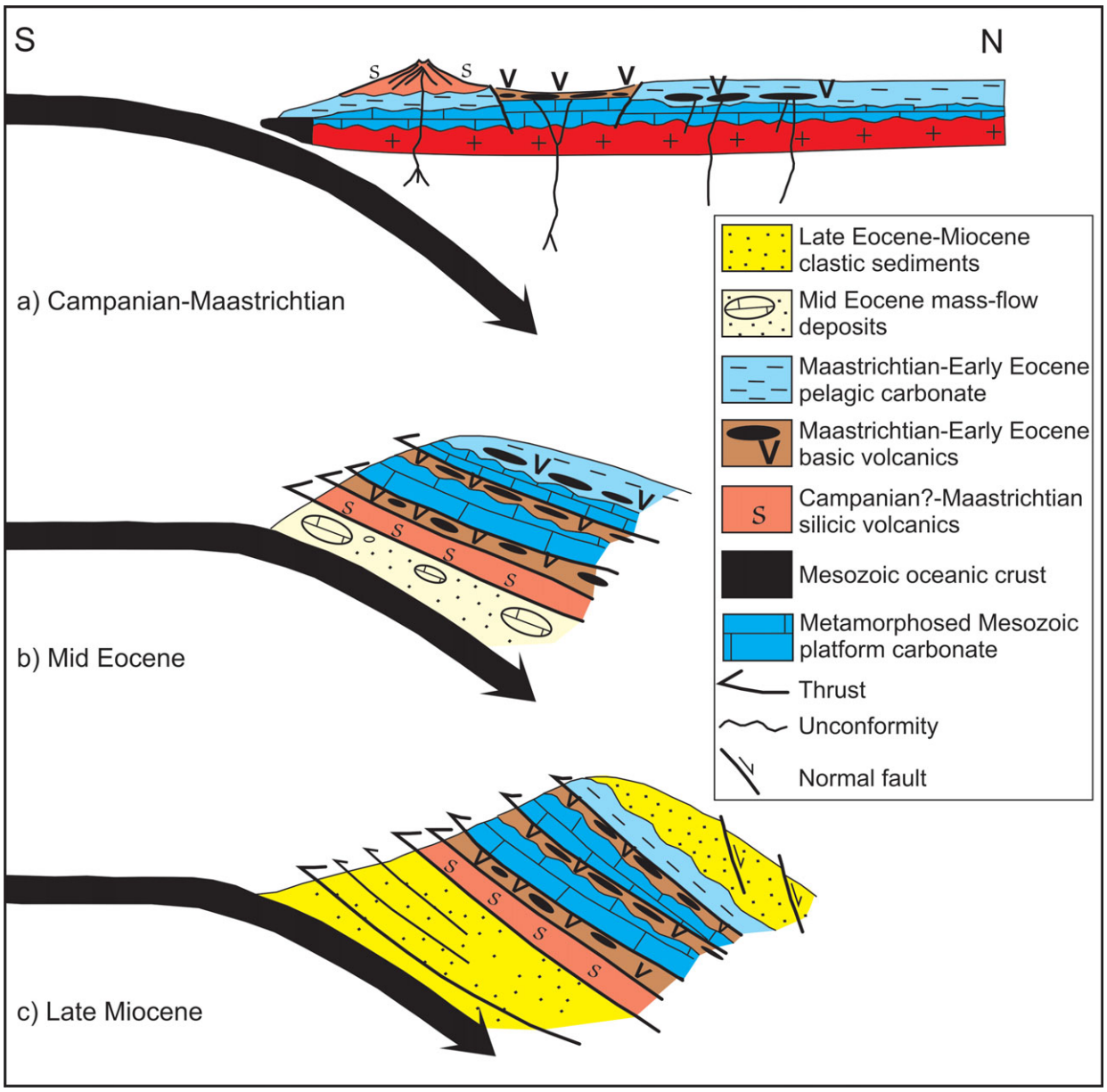

Figure 14. (Colour online) Interpretation of the Late Cretaceous to Late Miocene development of the Kyrenia Range following Late Cretaceous metamorphism and exhumation (see Fig. 13). (a) The silicic volcanism took place in a frontal location with basic volcanism mainly further north. The carbonate breccias were eroded locally along extensional (or transtensional) faults and interbedded with background pelagic carbonate, whereas the sandstone turbidites (Kiparisso Vouno (Alevkaya Tepe) Member) were mainly supplied from further-removed areas of the northern continental margin of the Southern Neotethys (see Fig. 15). (b) The whole of the Kyrenia Range was affected by S-directed thrusting during Middle Eocene time, which can be interpreted as an accretionary prism (work in progress). (c) Further southward thrusting took place in Late Miocene–Early Pliocene time resulting in southward thrusting over mainly Oligocene–Miocene clastic sediments (Mesarya (Mesaoria) Gp). Some of these sediments were also interleaved with the older Kyrenia Range rocks near the structural base in the south. Upper Cretaceous magmatic rocks may therefore have been more abundant than the present limited outcrop and could have been removed or concealed by later thrusting.

Troodos ophiolite, reaching a thickness of ~ 750 m thick (Robertson, 1977) in western Cyprus. The Kannaviou Formation is dominated by alternating bentonitic clays, radiolarian mudstones and volcaniclastic sandstones. The sandstones contain abundant grains of basaltic andesite and silicic volcanic glass of inferred volcanic arc origin, based on electron microprobe data (Robertson, 1990). These sediments and their ophiolitic basement restore to a relatively more northerly position prior to their well-documented 90° anticlockwise rotation during Late Campanian–Early Eocene time (Clube, Creer & Robertson, 1985; Clube & Robertson, 1986; see Morris, 1996). The silicic volcanic rocks in the Kyrenia Range and the volcanogenic sediments in western Cyprus could both represent remnants of continental margin arc magmatism, mainly not exposed owing to the effects of later-stage subduction or collision along the northern, active margin of the Southern Neotethys. The Kannaviou Formation is dated as Campanian to earliest Maastrichtian(?) using radiolarians and planktonic foraminifera (Urquhart & Banner, 1994; see also Lord *et al*. 2000). Assuming

a correlation with the Kyrenia Range, this would be consistent with a Campanian age of the silicic volcanics, as suggested by limited Ar–Ar dating (K. Huang, unpub. M.Sc. thesis, Univ. Hong Kong, 2008).

There is also evidence of Late Cretaceous arc-type magmatism cutting the Tauride carbonate platform (Keban-Malatya unit) in SE Turkey (Perinçek & Kozlu, 1984; Yazgan & Chessex, 1991; Robertson *et al*. 2006, 2007; Parlak, 2006; Karaoğlan *et al*. 2010). Improved radiometric dating indicates a limited age span of ∼ 84–81 Ma (Early Campanian) (Rızaoğlu *et al*. 2009). The magmatism can be explained by northward subduction of the Southern Neotethys beneath a Tauride microcontinent to form an Andean-type magmatic arc.

Within the Misis-Andırın Range, northeast of the Kyrenia Range (Fig. 1), Mesozoic carbonate platform rocks and mélange are structurally underlain by a broken formation that locally retains an intact succession (up to ∼ 300 m thick) of massive basalt, pillow basalt, pillow breccia and matrix-supported volcaniclastic debris flows. The volcaniclastic sediments include vitric, lithic and crystal tuffs that are inferred to have been derived from a calc-alkaline volcanic arc (Floyd *et al.* 1992). Associated turbidites contain mixtures of terrigenous and magmatic detritus suggesting a continental margin rather than oceanic setting. The pillow basalts exhibit a mildly enriched subduction-related pattern with La/Nb ratios suggestive of a back-arc setting (Floyd *et al*. 1991). In different areas the volcanogenic rocks are interbedded with radiolarian sediments and pelagic carbonates of Campanian–Maastrichtian age (Robertson *et al*. 2004), or Campanian age (Kozlu, 1987) based on dating using planktonic foraminifera. Previous reports (Floyd *et al*. 1991, 1992) of a Miocene age for the volcanic rocks in the Misis-Andırın Range have not been substantiated. This was based on the apparent presence of intercalations of Miocene sediments. However, these Miocene sediments were later shown to be tectonically interleaved with the volcanics, related to Late Miocene thrusting (Robertson *et al*. 2004).

The evidence of a Campanian–Maastrichtian age of the Misis-Andırın Range volcanic rocks (Robertson *et al*. 2004) prompts a comparison with the Kyrenia Range basaltic rocks. The field relations of the Upper Maastrichtian basalts in the Karpas Peninsula are comparable with exposures in the Misis-Andırın Range. Instead of simply basalt–pelagic carbonate intercalations as seen throughout the western, central and eastern range, exposures in the Karpas Peninsula include intercalations of red shale, radiolarites and calciturbidites (G. McCay, unpub. Ph.D. thesis, Univ., Edinburgh, 2010).

However, the Maastrichtian basalts in the Karpas Peninsula lack a subduction influence (Robertson & Woodcock, 1986; Huang, Malpas & Xenophontos, 2007; see also K. Huang, unpub. M.Sc. thesis, Univ. Hong Kong, 2008) in contrast to the basalts of the Misis-Andırın Range (Floyd *et al*. 1991, 1992).

One possibility is that the basaltic volcanism along the northern active margin was compositionally variable, related to melting of inhomogeneous mantle lithosphere that was variably affected by subduction and or extension (transtension?) during Late Cretaceous (Campanian–Maastrichtian) time.

6.b. Comparable Palaeogene magmatism

There is also evidence of Early–Mid-Eocene magmatism stretching from the Misis-Andırın Range eastwards into Iran. Eocene andesitic volcanic rocks with a subduction-related signature are locally exposed near the front of the over-riding Tauride thrust sheets, for example along the southern front of the Engizek Mountains (Yılmaz, 1993; Robertson *et al*. 2006). These volcanic rocks are chemically dissimilar to the Upper Paleocene–Middle Eocene variably 'enriched' basalts of the Kyrenia Range. On the other hand, further east along the Tauride thrust front, Eocene basalts erupted in a relatively deep-marine setting above metamorphic rocks in the Bitlis Massif (Karadere Volcanics; Aktaş & Robertson, 1984, 1990). Chemically, these are high-alumina basalts without evidence of a subduction influence and are chemically similar to some of the Upper Paleocene–Middle Eocene Kyrenia Range basalts. Eocene basaltic volcanics also erupted widely further north in eastern Turkey within a deep-marine setting, known as the Maden basin, as exposed in the Engizek-Pütürge and Bitlis massifs. The field relations of these basalts are indicative of an extensional setting, with a subduction chemical influence (Yılmaz, 1993; Robertson *et al*. 2006, 2007), similar to some of the Kyrenia Range Upper Paleocene–Middle Eocene basalts. There is also some evidence of Eocene granitic magmatism cutting the Malatya platform that is likely to be subduction-related based on recent radiometric age dating and chemical analysis (Parlak, 2006; Karaoğlan *et al*. 2010). The Middle Eocene magmatic rocks in southeastern Turkey can be interpreted as the result of northward subduction of a remnant Southern Neotethys resulting in small volumes of calc-alkaline magmatism, while within-plate volcanics with a subduction influence erupted in a back-arc setting further north (Robertson *et al*. 2006, 2007). Subduction was possibly oblique resulting in segmentation of the active margin into some parts undergoing subduction and calc-alkaline magmatism and others undergoing extension (or transtension) and related basaltic eruption (Aktaş & Robertson, 1990).

In general, the evidence from SE Turkey is indicative of Late Cretaceous northward subduction to form an Andean-type continental margin arc, apparently followed by magmatic quiescence until Middle Eocene time. This could relate to a period of arrested convergence of the Eurasian and African plates (Savostin *et al*. 1986). After subduction of the remaining oceanic crust during Eocene time, closure culminated in southward thrusting of the Taurides over the Arabian continental margin during Early Miocene

time (Perinçek & Özkaya, 1981; Yazgan & Chessex, 1993; Yılmaz, 1993; Robertson *et al*. 2006).

7. Late Cretaceous–Palaeogene tectonic development of the Kyrenia Range

In the light of the discussion in the previous Section, there are two main alternative possible settings for the basaltic volcanism of Late Maastrichtian and Late Paleocene–Middle Eocene ages in the Kyrenia Range.

The first assumes that some oceanic crust remained between the Kyrenia active margin and the Troodos ophiolite to the south during latest Cretaceous to Mid-Eocene time (see Savostin *et al*. 1986; Morris, 2003). Subduction of remnant oceanic crust fuelled Late Cretaceous and Late Paleocene to Middle Eocene volcanism along a long-lived Kyrenia active margin. The silicic volcanism of the western range and the Kannaviou volcanogenic sediments in western Cyprus reflect the development of a Campanian–Early Maastrichtian(?) volcanic arc. The Upper Maastrichtian and Upper Paleocene–Middle Eocene basaltic volcanic rocks erupted in a back-arc basin in this interpretation. The frontal arc straddled the continent–ocean boundary and was later mainly subducted or concealed by thrusting.

In the second interpretation, northward subduction again gave rise to Campanian–Early Maastrichtian(?) arc magmatism. However, this was short-lived and volumetrically minor. The Late Maastrichtian and Late Paleocene–Middle Eocene volcanism instead relates to the well-known anticlockwise palaeorotation of the Troodos microplate (Moores & Vine, 1971; Clube & Robertson, 1986; Robertson, 1990; Morris, 1996; Fig. 15). Recent palaeomagnetic work shows that the Troodos microplate included the Hatay ophiolite further east (Inwood *et al*. 2009). During subduction the Troodos microplate was carried northwards until it reached the Kyrenia active margin. The Troodos ophiolite then underwent anticlockwise rotation during Late Campanian–Early Eocene time (Clube, Creer & Robertson, 1985; Clube & Robertson, 1986; Morris, Creer & Robertson, 1990; Morris, 1996; Morris *et al*. 2006; Inwood *et al*. 2009). One scenario is that young, buoyant supra-subduction zone-type Troodos oceanic lithosphere subducted northwards beneath the Kyrenia active margin, failed to subduct, and then rotated anticlockwise. Recent palaeomagnetic work suggests that the Kyrenia Range experienced only limited, localized palaeorotation, possibly during Neogene time (Hodgson *et al*. 2010). The microplate boundary was, therefore, located between the Kyrenia continental margin and the Troodos ophiolite. The microplate rotation re-activated the Kyrenia margin in an extensional (or transtensional) setting triggering the 'enriched' within-plate-type volcanism in the Kyrenia Range with a variable inherited subduction signature.

In summary, linking the Late Maastrichtian and the Late Paleocene–Middle Eocene basaltic volcanism with the palaeorotation of the Troodos microplate appears to be the more plausible of the two hypotheses (Fig. 15).

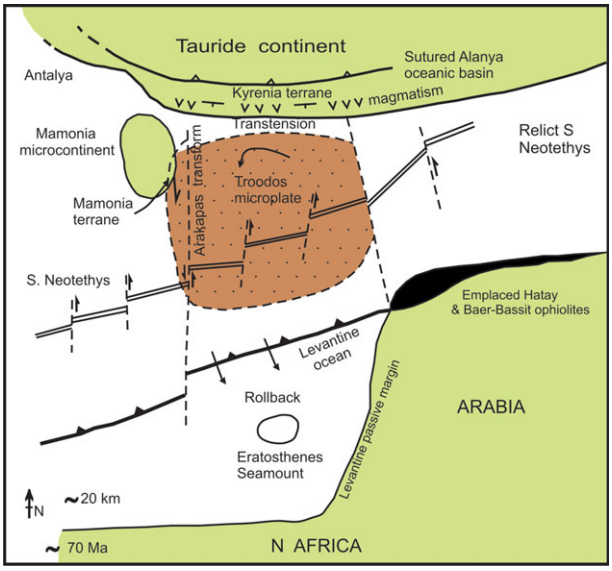

Figure 15. (Colour online) Plate tectonic interpretation showing the possible relation of the Kyrenia Range (Kyrenia terrane) to the anticlockwise rotation of the Troodos microplate during Late Cretaceous–Palaeogene time. Based on Robertson (1990) and Inwood *et al*. (2009). In an alternative tectonic model some oceanic crust still remained between the microplate and the Kyrenia margin; see text for explanation.

8. Conclusions

(1) The Mesozoic carbonate platform of the Kyrenia Range in the northern part of Cyprus is separated from an Upper Maastrichtian–Palaeogene succession by an important unconformity that is best exposed in the western and central Kyrenia Range.

(2) The Mesozoic carbonate platform was recrystallized and metamorphosed under greenschist-facies conditions probably during pre-Late Maastrichtian time.

(3) Metamorphosed and brecciated Mesozoic carbonate platform rocks were exhumed to the seafloor, coupled with subaqueous mass wasting of meta-carbonate talus. The seafloor was covered with pelagic carbonates in a relatively deep-water setting during Late Maastrichtian time.

(4) A previously enigmatic mixed carbonate–terrigenous–volcaniclastic interval, known only locally in the central Kyrenia Range represents an intercalation of relatively fine-grained sandy turbidites within transgressive Upper Maastrichtian pelagic carbonates. The source rocks were meta-carbonates, schistose rocks, basic volcanics and both neritic and pelagic carbonates. The turbidites were probably derived from outside the Kyrenia Range, possibly from adjacent parts of the northern continental margin of the Southern Neotethys.

(5) Two contrasting Upper Cretaceous volcanogenic sequences are exposed mainly in the western Kyrenia Range, separated by a low-angle thrust contact. The

structurally lower sequence of probable Campanian–Early Maastrichtian(?) age is dominated by pelagic carbonates, passing upwards into silicic tuffs and then into volcanogenic debris flows, followed by silicic lava flows. The silicic volcanogenic sequence is cross-cut by small alkaline basic intrusions. The overlying volcanic sequence is made up of basaltic pillow lavas, lava breccias and hyalotuff, interbedded with Upper Maastrichtian pelagic carbonates. Middle Eocene pelagic carbonates and basalts occur above this.

(6) Elsewhere, in the eastern Kyrenia Range and the Karpas Peninsula, thick sequences of pillow basalts erupted mainly during Late Maastrichtian time, followed by further basaltic volcanism during Late Paleocene–Middle Eocene time.

(7) The suggested tectonic scenario is one involving Late Cretaceous (Late Santonian–Campanian) northward subduction of the Southern Neotethys. The Mesozoic Kyrenia carbonate platform was located on the subducting plate and was underthrust beneath a larger Tauride microcontinent to the north in this interpretation. This was followed by extensional exhumation, accumulation of meta-carbonate rock talus and transgression by pelagic carbonates.

(8) Basaltic volcanic rocks of variably 'enriched' and more 'depleted' composition erupted along the deeply submerged northern continental borderland of the Southern Neotethys probably in an extensional or transtensional setting during discrete Late Maastrichtian and Late Paleocene–Middle Eocene time intervals.

(9) The silicic volcanism in the Kyrenia Range can probably be correlated with the Campanian tuffaceous sediments of the Kannaviou Formation in western Cyprus.

(10) The Late Cretaceous Kyrenia active margin can also be correlated with the active continental margin of the Tauride continent further east in SE Turkey, where comparable mainly Campanian arc-type rocks are exposed. Palaeogene (mainly Middle Eocene) magmatism characterizes both regions.

(11) The Late Cretaceous–Palaeogene tectonic development and magmatism of the Kyrenia Range is likely to have been influenced by the anticlockwise rotation of the Troodos microplate.

Acknowledgements. John Dixon, Gillian McCay, Mark Anderson, Tony Morris and Mehmet Necdet are thanked for discussion. Mustafa Alkaravli is also thanked for providing the logistical support of the Geology and Minerals Department during this work. Constructive review helped us to improve the paper, including advice from the editor, Dr Mark Allen. We thank Dr Hayati Koç for assistance with preparing figures.

References

AKTAŞ, G. & ROBERTSON, A. H. F. 1984. The Maden Complex, S E Turkey: evolution of a Neotethyan continental margin. In *The Geological Evolution of the Eastern Mediterranean* (eds J. E. Dixon & A. H. F. Robertson), pp. 375–402. Geological Society of London, Special Publication no. 17.

AKTAŞ, G. & ROBERTSON, A. H. F. 1990. Tectonic evolution of the Tethys suture zone in S.E. Turkey: evidence from the petrology and geochemistry of Late Cretaceous and Middle Eocene extrusives. In *Ophiolites – Oceanic Crustal Analogues: Proceedings of the International Symposium 'Troodos 1987'* (eds E. M. Moores, A. Panayiotou & C. Xenophontos), pp. 311–29. Nicosia, Cyprus: Geological Survey Department.

AL-RIYAMI, K., ROBERTSON, A. H. F., XENOPHONTOS, C. & DIXON, J. E. 2002. Origin and emplacement of the Late Cretaceous Baer-Bassit ophiolite and its metamorphic sole in NW Syria. *Lithos* **65**, 225–60.

BAROZ, F. 1979. *Etude géologique dans le Pentadaktylos et la Mesaoria (Chypre Septentrionale)*. Published Docteur D'Etat Thesis. Université de Nancy France, vols. 1 & 2.

BAROZ, F. 1980. Volcanism and continent-island arc collision in the Pentadaktylos range, Cyprus. In *Ophiolites: Proceedings of the International Symposium 'Troodos 1979'* (ed. A. Panayiotou), pp. 73–5. Nicosia, Cyprus: Geological Survey Department.

BARRIER E. & VRIELYNCK B. (eds) 2009. *Palaeotectonic Maps of the Middle East*. Paris: Middle East Basins Evolution Programme.

CLEINTUAR, M. R., KNOX, G. J. & EALEY, P. J. 1977. The geology of Cyprus and its place in the East-Mediterranean framework. *Geologie en Mijnbouw* **56**, 66–82.

CLUBE, T. M. M., CREER, K. M. & ROBERTSON, A. H. F. 1985. The palaeorotation of the Troodos microplate. *Nature* **317**, 522–5.

CLUBE, T. M. M. & ROBERTSON, A. H. F. 1986. The palaeorotation of the Troodos microplate, Cyprus, in the Late Mesozoic-Early Cenozoic plate tectonic framework of the Eastern Mediterranean. *Surveys in Geophysics* **8**, 375–437.

DERCOURT, J., ZONENSHAIN, L.-P., RICOU, L. E., KAZMIN, V. G., LE PICHON, X., KNIPPER, A. L., GRANDJACQUET, C., SBORTSHIKOV, I. M., GEYSSANT, J., LEPVRIER, C., PECHIERSKY, D. H., BOULIN, J., SIBUET, J. C., SAVOSTIN, L. A., SOROKHTIN, O., WESTPHAL, M., BAZHENOV, M. L., LAUER, J. P. & BIJUDUVAL, B. 1986. Geological evolution of the Tethys belt from the Atlantic to the Pamirs since the Lias. *Tectonophysics* **123**, 241–315.

DERCOURT, J., GAETANI, M., VRIELYNCK, B., BARRIER, E., BIJU-DUVAL, B., BRUNET, M. F., CADET, J. P., CRASQUIN, S. & SANDULESCU, M. 2000. *Peri-Tethys Palaeogeographical Atlas 2000*. Paris: Commission de la Carte Géologique du Monde/Commission for the Geologic Map of the World.

DUCLOZ, C. 1972. The Geology of the Bellapais-Kyrthrea Area of the Central Kyrenia Range. *Cyprus Geological Survey Bulletin* **6**, 75 pp.

FLOYD, P. A., KELLING, G., GÖKÇEN, S. L. & GÖKÇEN, N. 1991. Geochemistry and tectonic environment of basaltic rocks from the Misis ophiolitic melange, South Turkey. *Chemical Geology* **89**, 263–79.

FLOYD, P. A., KELLING, G. & GÖKÇEN, S. L. & GÖKÇEN, N. 1992. Arc-related origin of volcaniclastic sequences in the Misis Complex, Southern Turkey. *Journal of Geology* **100**, 221–30.

GASS, I. G. 1990. Ophiolites and ocean lithosphere. In *Ophiolites – Oceanic Crustal Analogues: Proceedings of the International Symposium 'Troodos 1987'* (eds J. Malpas, E. M. Moores, A. Panayiotou & C. Xenophontos), pp. 1–12. Nicosia, Cyprus: Geological Survey Department.

HAKYEMEZ, A. & ÖZKAN-ALTINER, S. 2007. Beşparmak Dağları'ndaki (Kuzey Kıbrıs) Üst Maastrihtiyen-Eosen ıstifinin planktonik foraminifer biyostratigrafisi (Planktonic foraminiferal biostratigraphy of the Upper Maastrichtian–Eocene sequence in the Beşparmak Range, Northern Cyprus). In *60th Geological Congress of Turkey, Ankara, Abstract Book*, pp. 416–19.

HAKYEMEZ, Y., TURHAN, N., SÖNMEZ, İ. & SÜMENGEN, M. 2000. *Kuzey Kıbrıs Türk Cumhuriyeti'nin Jeolojisi* (Geology of the Northern Cyprus Turkish Republic). Ankara: Mineral Research and Exploration Institute of Turkey, Report, 44 pp.

HARRISON, R. W., NEWELL, W. L., BATIHANLI, H., PANAYIDES, I., MCGEEHIN, J. P., MAHAN, S. A., OZHUR, A., TSIOLAKIS, E. & NECDET, M. 2004. Tectonic framework and Late Cenozoic tectonic history of the northern part of Cyprus: implications for earthquake hazards and regional tectonics. *Journal of Asian Earth Sciences* **23**, 191–210.

HENSON, F. R. S., BROWNE, R. V. & MCGINTY, J. 1949. A synopsis of the stratigraphy and geological history of Cyprus. *Quarterly Journal of the Geological Society of London* **CV**, 2–37.

HODGSON, E., MORRIS, A., ANDERSON, M. & ROBERTSON, A. 2010. *First Palaeomagnetic Results From the Kyrenia Range Terrane of Northern Cyprus*. Vienna: European Union of Geosciences. Published abstract.

HUANG, K., MALPAS, J. & XENOPHONTOS, C. 2007. Geological studies of igneous rocks and their relationships along the Kyrenia Range. In *Abstracts of the 6th International Congress of Eastern Mediterranean Geology, 2–5 April, 2007, Amman, Jordan* (eds K. Moumani, K. Shawabkeh, A. Al-Malabeh & M. Abdelghafoor), p. 53.

INWOOD, J., MORRIS, A., ANDERSON, M. W. & ROBERTSON, A. H. F. 2009. Neotethyan intraoceanic microplate rotation and variations in spreading axis orientation: palaeomagnetic evidence from the Hatay ophiolite (southern Turkey). *Earth and Planetary Science Letters* **280**, 105–17.

KARAOĞLAN, F., PARLAK, O., HEJL, E., NEUBAUER, F., KLÖTZLI, U., KOLLER, F. & KOP, A. 2010. The temporal evolution of arc magmatisms beneath the Tauride active continental margin. In *Abstract Book, 7th International Symposium on Eastern Mediterranean Geology, 18–22 October, 2010, Adana, Turkey* (eds S. Bozdağ, T. Çan & F. Karaoğlan), p. 7.

KELLING, G., GÖKÇEN, S. L., FLOYD, P. A. & GÖKÇEN, N. 1987. Neogene tectonics and plate convergence in the eastern Mediterranean: new data from southern Turkey. *Geology* **15**, 425–9.

KEMPLER, D. 1998. Eratosthenes Seamount: the possible spearhead of incipient continental collision in the Eastern Mediterranean In *Proceedings of the Ocean Drilling Program, Scientific Results, vol. 160* (eds A. H. F. Robertson, K.-C. Emeis, K. C. Richter & A. Camerlenghi), pp. 709–21. College Station, Texas.

KEMPLER, D. & GARFUNKEL, Z. 1994. Structures and kinematics in the northeastern Mediterranean: a study of an irregular plate boundary. *Tectonophysics* **234**, 19–32.

KOZLU, H. 1987. Structural development and stratigraphy of Misis–Andırın region. In *Proceedings of the Seventh Turkish Petroleum Congress, Ankara*, pp. 104–16 (in Turkish with an English abstract).

LORD, A. R., PANAYIDES, A., URQUHART, E. & XENOPHONTOS, C. 2000. A biostratigraphical framework for the Late Cretaceous–Recent circum-Troodos sedimentary sequence, Cyprus. In *Proceedings of the Third International Conference on the Geology of the Eastern Mediterranean* (eds I. Panayides, C. Xenophontos & J. Malpas), pp. 289–98. Nicosia, Cyprus: Geological Survey Department.

MOORE, T. A. 1960. *The Geology and Mineral Resources of the Astromeritis-Kormakiti Area*. Nicosia, Cyprus: Geological Survey Department, Memoir 6, 96 pp.

MOORES, E. M. & VINE, F. J. 1971. The Troodos Massif, Cyprus and other ophiolites as oceanic crust: evaluations and implications. *Philosophical Transactions of the Royal Society* **A268**, 433–66.

MORRIS, A. 1996. A review of palaeomagnetic research in the Troodos ophiolite, Cyprus. In *Palaeomagnetism and Tectonics of the Mediterranean Region* (eds A. Morris & D. Tarling), pp. 311–24. Geological Society of London, Special Publication no. 105.

MORRIS, A. 2003. The Late Cretaceous palaeolatitude of the Neotethyan spreading axis in the eastern Mediterranean region. *Tectonophysics* **377**, 157–78.

MORRIS, A., ANDERSON, M. W., INWOOD, J. & ROBERTSON, A. H. F. 2006. Palaeomagnetic insights into the evolution of Neotethyan oceanic crust in the eastern Mediterranean. In *Tectonic Development of the Eastern Mediterranean Region* (eds A. H. F. Robertson & D. Mountrakis), pp. 351–72. Geological Society of London, Special Publication no. 260.

MORRIS, A., CREER, K. M. & ROBERTSON, A. H. F. 1990. Palaeomagnetic evidence for clockwise tectonic rotations related to dextral shear along the Southern Troodos Transform Fault, Cyprus. *Earth and Planetary Science Letters* **99**, 250–62.

MUSAKA, S. B. & LUDDEN, J. N. 1987. Uranium-lead ages of plagiogranites from the Troodos ophiolite, Cyprus, and their tectonic significance. *Geology* **15**, 825–8.

OKAY, A. I. 1989. An exotic eclogite/blueschist slice in a Barrovian-style metamorphic terrain, Alanya Nappes, southern Turkey. *Journal of Petrology* **30**, 107–32.

OKAY, A. I. & ÖZGÜL, N. 1984. HP/LT metamorphism and the structure of the Alanya Massif, Southern Turkey: an allochthonous composite tectonic sheet. In *The Geological Evolution of the Eastern Mediterranean* (eds J. E. Dixon & A. H. F. Robertson), pp 415–29. Geological Society of London, Special Publication no. 17.

PARLAK, O. 2006. Geodynamic significance of granitoid magmatism in southeast Anatolia: geochemical and geochronological evidence from the Göksun–Afşin (Kahranmanmaraş, Turkey) region. *International Journal of Earth Sciences* **95**, 609–27.

PARLAK, O., HÖCK, V., KOZLU, H. & DELALOYE, M. 2004. Oceanic crust generation in an island arc tectonic setting, SE Anatolian Orogenic belt (Turkey). *Geological Magazine* **141**, 583–603.

PEARCE, J. A. 1975. Basalt geochemistry used to investigate past tectonic environments in Cyprus. *Tectonophysics* **25**, 41–67.

PERINÇEK, D. & KOZLU, H. 1984. Stratigraphical and structural relations of the units in the Afşin-Elbistan-Doğanşehir region (Eastern Taurus). In *Geology of the Taurus Belt: Proceedings of the International Symposium, MTA, Ankara* (eds O. Tekeli & M. C. Göncüoğlu), pp. 181–98.

PERINÇEK, D. & ÖZKAYA, I. 1981. Tectonic evolution of the northern margin of the Arabian plate. *Yerbilimleri, Bulletin of the Institute of Earth Sciences of Hacettepe University* **8**, 91–101.

RIZAOĞLU, T., PARLAK, O., HÖCK, V., KOLLER, F., HAMES, W. E. & BILLOR, Z. 2009. Andean-type active margin formation in the eastern Taurides: geochemical and

geochronological evidence from the Baskil granitoid (Elazığ, SE Turkey). *Tectonophysics* **473**, 188–207.

ROBASZYNSKI, F. & CARON, M. 1995. Foraminifères planktoniques du Crétacé: commentaire de la zonation Europe-Méditerranée. *Bulletin de la Societé Géologique de France* **166** (6), 681–92.

ROBERTSON, A. H. F. 1977. The Kannaviou Formation Cyprus: volcaniclastic sedimentation from a probable Late Cretaceous island arc. *Journal of the Geological Society, London* **134**, 269–92.

ROBERTSON, A. H. F. 1990. Tectonic evolution of Cyprus. In *Ophiolites – Oceanic Crustal Analogues: Proceedings of the International Symposium 'Troodos 1987'* (eds E. M. Moores, A. Panayiotou & C. Xenophontos), pp. 235–250. Nicosia, Cyprus: Geological Survey Department.

ROBERTSON, A. H. F. 1993. Mesozoic–Tertiary sedimentary and tectonic evolution of Neotethyan carbonate platforms, margins and small ocean basins in the Antalya Complex, S.W. Turkey. In *Tectonic Controls and Signatures in Sedimentary Successions* (eds L. Frostick & R. Steel), pp. 415–65. Special Publication of the International Association of Sedimentologists, no. 20.

ROBERTSON, A. H. F. 1998. Mesozoic–Cenozoic tectonic evolution of the easternmost Mediterranean area: integration of marine and land evidence. In *Proceedings of the Ocean Drilling Program, Scientific Results, vol. 160* (eds A. H. F. Robertson, K.-C. Emeis, K. C. Richter & A. Camerlenghi), pp. 723–82. College Station, Texas.

ROBERTSON, A. H. F. & DIXON, J. E. 1984. Introduction; Aspects of the Geological Evolution of the Eastern Mediterranean. In *The Geological Evolution of the Eastern Mediterranean* (eds J. E. Dixon & A. H. F. Robertson), pp. 1–74. Geological Society of London, Special Publication no. 17.

ROBERTSON, A. H. F., PARLAK, O., RIZAOĞLU, T., UNLÜGENÇ, U., İNAN, N., TASLI, K. & USTAÖMER, T. 2007. Tectonic evolution of the South Tethyan ocean: evidence from the Eastern Taurus Mountains (Elazığ region, SE Turkey). In *Deformation of the Continental Crust: The Legacy of Mike Coward* (eds A. C. Ries, R. W. H. Butler & R. H. Graham), pp. 231–70. Geological Society of London, Special Publication no. 272.

ROBERTSON, A. H. F., UNLÜGENÇ, Ü. C., İNAN, N. & TASLI, K. 2004. The Misis–Andırın Complex: a Mid-Tertiary melange related to late-stage subduction of the Southern Neotethys in S Turkey. *Journal of Asian Earth Sciences* **22**, 413–53.

ROBERTSON, A. H. F., USTAÖMER, T., PARLAK, O., UNLÜGENÇ, U. C., TASLI, K. & İNAN, N. 2006. The Berit transect of the Tauride thrust belt, S Turkey: Late Cretaceous–Early Cenozoic accretionary/collisional processes related to closure of the Southern Neotethys. *Journal of Asian Earth Sciences* **27**, 108–45.

ROBERTSON, A. H. F. & WOODCOCK, N. H. 1986. The role of the Kyrenia Range lineament, Cyprus, in the geological evolution of the Eastern Mediterranean area. In *Major Crustal Lineaments and their Influence on the Geological History of the Continental Lithosphere* (eds H. G. Reading, J. Watterson & S. H. White), pp. 141–71. *Philosophical Transactions of the Royal Society of London, Series A*, **317**.

ROBERTSON, A. H. F. & XENOPHONTOS, C. 1993. Development of concepts concerning the Troodos ophiolite and adjacent units in Cyprus. In *Magmatic Processes and Plate Tectonics* (eds H M. Prichard, T. Alabaster, N. B. Harris & C. R. Neary), pp. 85–120. Geological Society of London, Special Publication no. 70.

ROBINSON, P. T. & MALPAS, J. 1990. The Troodos Ophiolite of Cyprus: new perspectives on its origin and emplacement. In *Ophiolites – Oceanic Crustal Analogues: Proceedings of the International Symposium 'Troodos 1987'* (eds E. M. Moores, A. Panayiotou & C. Xenophontos), pp.13–36. Nicosia, Cyprus: Geological Survey Department.

SARTORIO, D. & VENTURINI, S. 1988. *Southern Tethys Biofacies*. S. Donato, Milanese: Agip S.p.A., 235 pp.

SAVOSTIN, L. A., SIBUET, J. C., ZONENSHAIN, L. P., LE PICHON, X. & ROLET, J. 1986. Kinematic evolution of the Tethys belt, from the Atlantic to the Pamirs since the Triassic. *Tectonophysics* **123**, 1–35.

STAMPFLI, G. M. & BOREL, G. D. 2002. A plate tectonic model for the Palaeozoic and Mesozoic constrained by dynamic plate boundaries and restored synthetic oceanic isochrones. *Earth and Planetary Science Letters* **169**, 17–33.

URQUHART, E. & BANNER, F. T. 1994. Biostratigraphy of the supra-ophiolite sediments of the Troodos Massif, Cyprus: the Cretaceous Perapedhi, Kannaviou, Moni and Kathikas formations. *Geological Magazine* **131**, 499–518.

YAZGAN, E. & CHESSEX, R. 1991. Geology and tectonic evolution of the Southeastern Taurides in the region of Malatya. *Bulletin of the Turkish Association of Petroleum Geologists* **3** (1), 1–42.

YILMAZ, Y. 1993. New evidence and model on the evolution of the southeast Anatolian orogen. *Geological Society of America Bulletin* **105**, 251–71.

ZITTER, T. A. C., WOODSIDE, J. M. & MASCLE, J. 2003. The Anaximander Mountains: a clue to the tectonics of southwest Anatolia. *Geological Journal* **38**, 375–94.

Appendix

Table A1. Upper Cretaceous location data

Sample no.	Location and GPS coordinates
06/10a	Geçiköy (Panagra Gorge), west side of road cutting, GPS 0506455 3910696;
06/11a	Karşıyaka (Vasileia), GPS 0510458 3910789;
06/31b	Ergenekon (Ayios Chariton), GPS 0555395 3907578;
06/21b	Balalan (Platanisso), GPS 0601072 3927147;
06/29b	Ağıllar (Mandres) GPS 0572536 3912378;
06/30	Ağıllar (Mandres) GPS 0574635 3912220;
09/40	Kayalar (Orga), hillside above road;
249	Balalan (Platanisso), thrust sheet of redeposited pelagic limestone; in the middle of the Balalan lava massif;
06/3a	Tirmen (Trypimeni) GPS 0559063 3909593;
06/4a	Tirmen (Trypimeni) GPS 0557866 3909552;
06/8a	Çınarlı (Platani) GPS 0569468 3910646;
06/10b	Geçiköy (Panagra Gorge), west side of road cutting, GPS near 0506455 3910696;
06/11b	Karşıyaka (Vasileia), GPS 0510458 3910789;
06/11d	Karşıyaka (Vasileia), GPS near 0510458 3910789;
06/21a	Balalan (Platanisso) GPS 0601072 3927147;
06/ 27a	North flank of the Balalan (Platanisso) lava massif;
09/41	Kayalar (Orga), hillside above road;
09/47	Kayalar (Orga), hillside above road;
06/2a	Mallıdağ (Melounda) GPS 0563212 3910902;
06/17a–c,e	Balalan (Platanisso) GPS 0600275 3926976;
06/28a,b	Değirmenlik (Kithrea) GPS 0541410 3903223;
06/11c	Karşıyaka (Vasileia), near GPS 0510458 3910789;
06/17d	Balalan (Platanisso) GPS near 0600275 3926976;
06/21c	Balalan (Platanisso) GPS near 0601072 3927147;
06/2c	Mallıdağ (Melounda) GPS near 0563212 3910902;
06/1a	Mallıdağ (Melounda) GPS 0563064 3910753;
06/29a	Ağıllar (Mandres) GPS 0572536 3912378;
06/31a	Ergenekon (Ayios Chariton) GPS 0555395 3907578;
06/28	Değirmenlik (Kithrea) GPS 0541410 3903223;
250	Balalan (Platanisso), thrust sheet of redeposited pelagic limestone; in the middle of the Balalan lava massif;
09/21	Beylerbey (Bellapais); stream section SE of village (Baroz, 1979 location);
09/32	Geçiköy (Panagra Gorge), hillside east of road cutting;
09/18–19	Beylerbey (Bellapais); hill section SE of village (see text);
06/26a	North flank of the Balalan (Platanisso) lava massif.

The locations of samples are also shown on the local maps. GPS locations use ED 1950 coordinates.

Table A2. Cenozoic location data

Sample no.	Location and GPS coordinates
06/5a,b,c	Tirmen (Trypimeni) GPS 0556673 3909222;
06/9a	Çınarlı (Platani) GPS 0576783 3907578;
09/24	Beylerbey (Bellapais); stream section SE of village (Baroz, 1979 location);
06/96	Geçiköy (Panagra); associated with basaltic lava in the east side of the main road near the top of the succession (beneath the Miocene transgression);
09/39	Kayalar (Orga), low on hillside ~20 m above road to S;
09/30	Çınarlı (Platani); high levels of sequence on E side of main road;
06/18a,b	Balalan (Platanisso), GPS 0600717 3927055;
09/23	Balalan (Platanisso), GPS 0600717 3927055.

The locations of samples are also shown on the local maps. GPS locations use ED 1950 coordinates.